Blood Phantom Concentration Measurement Using An I-Q Receiver Design

By

Matt Kitchen

B.Sc., University of Kansas, 2011

Submitted to the graduate degree program in Electrical Engineering and Computer Science (EECS) and the Graduate Faculty of the University of Kansas in partial fulfillment of the requirements

for the degree of Master of Science Electrical Engineering.

_____

Chair: Ron Hui

_____

Chris Allen

_____

Jim Stiles

Date Defended: 10 May 2018

The thesis committee for Matt Kitchen certifies that this is the approved version of the following thesis:

Blood Oxygenation Concentration Measurement Using An I-Q Receiver Design

_____

Chair: Ron Hui

Date Approved: 10 May 2018

Abstract

Near-infrared spectroscopy has been used as a non-invasive method of determining concentration of chemicals within living tissues of living organisms. This method employs LEDs of specific frequencies to measure concentration of blood constituents according to the Beer-Lambert Law. One group of instruments (frequency domain instruments) is based on amplitude modulation of the laser diode or LED light intensity, the measurement of light adsorption and the measurement of modulation phase shift to determine light path length for use in Beer-Lambert Law. This paper describes the design and demonstration of a frequency domain instrument for measuring concentration of oxygenated and de-oxygenated hemoglobin using incoherent optics and an in-phase quadrature (I-Q) receiver design. The design has been shown to be capable of resolving variations of concentration of test samples and a viable prototype for future, more precise, tools.

Table of Contents

Chapter I: Introduction

Motivation

In medical diagnosis procedures, blood oxygenation measurements have a wide variety of uses such as detection of brain oxygen asphyxia or lung disease. Near-infrared spectroscopy has been used as a non-invasive (not requiring incision or puncture of the skin) method of determining concentration of chemicals within living tissues of living organisms. The intent of this experiment is to explore the use of an in-phase and quadrature (I-Q) signal receiver design to measure hemoglobin oxygenation concentration. Using the Beer-Lambert law, chemical concentrations can be calculated using the optical path length difference and absorption; characteristics proportional to signal phase delay and signal amplitude respectively.

Near Infrared Spectroscopy (NIRS) has been adopted commercially as a method for non-invasive, in-vivo blood oxygen saturation measurement. Human body tissue is more nearly transparent to light in the near-infrared spectrum when compared to light in the visible spectrum. NIRS technology takes advantage of this characteristic of near-infrared light by measuring the absorption of light as passes through tissue. Most non-invasive methods employ laser diodes or LEDs of specific frequencies to measure concentration of blood constituents according to the Beer-Lambert Law. V O Rybynok and P A Kyriacou [1] present a light-tissue interaction theory, based on modern understanding of the behavior of light photons, toward better understanding of the Beer-Lambert Law. Adelina Pellicer and María del Carmen Bravo [2] present a review of the operating principles of equipment currently in use and operating principals which are in development. The primary methods presented are 1) NIRS continuous-wave (CW) instruments, 2) Time-of-flight or Time-Domain (TD) instruments, 3) Frequency-domain (FD) instruments, and 4) technologies that

are currently under development. The CW method is capable of measuring changes in blood oxygen saturation but this method has the disadvantage of not being capable of determining actual concentrations of oxygenated and deoxygenated hemoglobin. The TD and FD methods have the advantage of having the capability of measuring actual concentrations of oxygenated and deoxygenated hemoglobin. The TD instruments are large and expensive. The FD instruments have the potential of being smaller, less expensive and able to be used in vivo. This paper presents work toward the development of an instrument based on the frequency-domain method implementing an In-phase and Quadrature (I-Q) receiver design. Figure b (reproduced from [2]) illustrates the reduction in modulated light intensity (I) and phase shift (ϕ) of the modulation as the light passes through a tissue sample. Measurements of the change in light intensity and phase shift of modulation can be used to determine constituent concentration using the Beer-Lambert Law after optical path length difference is calculated using the modulation phase shift and attenuation is calculated using calculated signal amplitude.

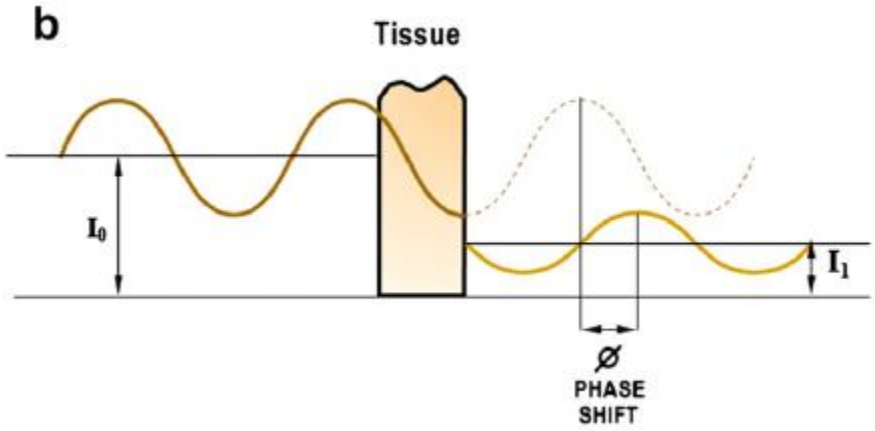

For more information regarding work in blood oxygenation measurement based on NIRS and the Beer-Lambert Law, refer to [3] [4] [5] [6] [7] .

Molar Absorptivity, Extinction Coefficients and Path Length Difference

This section presents the Beer-Lambert law as a means for calculating concentrations of oxygenated and deoxygenated blood using measured parameters of light from an In-Phase and Quadrature (I-Q) receiver. Beer-Lambert's Law (also known as Beer-Lambert-Bouguer Law) states that the absorbance of photons by a medium is proportional to the extinction coefficient, concentration of the medium and the optical path length difference. Equation (1) describes Beer-Lambert law for a single medium.

$$\alpha = log_{10}\left(\frac{I_0}{I}\right) = \epsilon c l \tag{1}$$

Where:

α is the absorbance, dimensionless

I_0 is the source light intensity, proportional to A_0 the electrical amplitude

I is the measured light intensity, proportional to A the electrical amplitude

ϵ is the extinction coefficient, $\left[\frac{liter}{mol*cm}\right]$

c is the concentration of the medium, $\left[\frac{mol}{liter}\right]$

ℓ is the optical path length difference in the medium, [cm]

The extinction coefficient of the medium is wavelength dependent, thus Equation (1) can be represented as follows.

$$\alpha(\lambda) = \epsilon(\lambda) c \ell \tag{2}$$

Equation (2) represents the absorption of light, of a specified wavelength, in a single homogenous medium. The Beer-Lambert Law can be expanded to represent the absorption of a heterogeneous medium, where λ_i is the wavelength of light incident on the medium.

$$\alpha(\lambda_i) = \ell \sum_{j=1}^{N} \epsilon_j(\lambda_i) c_j \quad (3)$$

In blood, oxygenated and deoxygenated hemoglobin are present, and the absorption of light at 650 and 820 nm by each of the constituents can be expressed as follows.

$$\alpha(\lambda = 650\,nm) = [\epsilon_{HbO_2}(\lambda = 650\,nm) * c_{HbO_2} + \epsilon_{Hb}(\lambda = 650\,nm) * c_{Hb}]\ell_{650\,nm} \quad (4)$$

$$\alpha(\lambda = 820\,nm) = [\epsilon_{HbO_2}(\lambda = 820\,nm) * c_{HbO_2} + \epsilon_{Hb}(\lambda = 820\,nm) * c_{Hb}]\ell_{820\,nm} \quad (5)$$

Where:

ϵ_{HbO_2} is the extinction coefficient of oxygenated hemoglobin, $\left[\frac{liter}{mol*cm}\right]$

c_{HbO_2} is the concentration of oxygenated hemoglobin, $\left[\frac{mol}{liter}\right]$

ϵ_{Hb} is the extinction coefficient of deoxygenated hemoglobin, $\left[\frac{liter}{mol*cm}\right]$

c_{Hb} is the concentration of deoxygenated hemoglobin, $\left[\frac{mol}{liter}\right]$

A prototype system was designed to measure path length and absorption of incident photons, in order to determine the concentration of oxygenated and deoxygenated hemoglobin, which are represented by c_{HbO_2} and c_{Hb} in Equations (4) and (5). The extinction coefficients ϵ_{HbO_2} and ϵ_{Hb} in Equations (4) and (5) are known values for oxygenated and deoxygenated hemoglobin, respectively, from extinction coefficient data gathered by Prahl [8]. These values for the extinction coefficient of oxygenated and deoxygenated hemoglobin are shown in Table 1.

Table 1 - Known Extinction Coefficients of Oxygenated and Deoxygenated Hemoglobin

Extinction Coefficient	$\left(\frac{\boldsymbol{liter}}{\boldsymbol{mol * cm}}\right)$
$\epsilon_{\mathrm{HbO_2}}(\lambda = 650\,nm)$	368

$\epsilon_{\mathrm{Hb}}(\lambda = 650\ nm)$	3750.12
$\epsilon_{\mathrm{HbO_2}}(\lambda = 820\ nm)$	916
$\epsilon_{\mathrm{Hb}}(\lambda = 820\ nm)$	693.76

With these values known, the variables necessary to calculate the values for concentration are the absorption coefficient A and path length ℓ at 650 and 820 nm. Therefore, the concentration can be solved for with the following equations, where the absorption, extinction coefficient and path length are either known, measured, or calculated based upon measurement. Solving Equations (4) and (5) for the concentration of oxygenated and deoxygenated hemoglobin yields Equations (6) and (7) respectively.

$$c_{Hb} = \frac{\left[\frac{\alpha(\lambda = 650nm)}{\ell_{650}} - \frac{\epsilon_{HbO_2}(\lambda = 650nm)\alpha(\lambda = 820nm)}{\epsilon_{HbO_2}(\lambda = 820nm)\ell_{820}}\right]}{\left[\epsilon_{Hb}(\lambda = 650nm) - \frac{\epsilon_{HbO_2}(\lambda = 650nm)\epsilon_{Hb}(\lambda = 820nm)}{\epsilon_{HbO_2}(\lambda = 820nm)}\right]} \tag{6}$$

$$c_{HbO_2} = \frac{\left[\frac{\alpha(\lambda = 820nm)}{\ell_{820}} - \frac{\epsilon_{Hb}(\lambda = 820nm)\alpha(\lambda = 650nm)}{\epsilon_{Hb}(\lambda = 650nm)\ell_{650}}\right]}{\left[\epsilon_{HbO_2}(\lambda = 820nm) - \frac{\epsilon_{Hb}(\lambda = 820nm)\epsilon_{HbO_2}(\lambda = 650nm)}{\epsilon_{Hb}(\lambda = 650nm)}\right]} \tag{7}$$

Absorption Spectrum of Hemoglobin

Oxygenated hemoglobin has less of an extinction coefficient at 650 nm, thus a reduced absorption of incident photons, when compared to deoxygenated hemoglobin at the same wavelength. The optical path length of infrared radiation in hemoglobin varies due to the concentration of oxygen in the hemoglobin. Figure 1 shows the extinction coefficient of hemoglobin on a logarithmic scale versus optical wavelength [8]. Figure 1 shows a range of wavelength larger than the spectrum necessary for distinction between the extinction coefficient of oxygenated and deoxygenated

hemoglobin. Figure 2 shows the extinction coefficient spectrum on a smaller scale. The vertical lines in Figure 2 are indicating the difference in absorption at the two wavelengths, 650 nm and 820 nm.

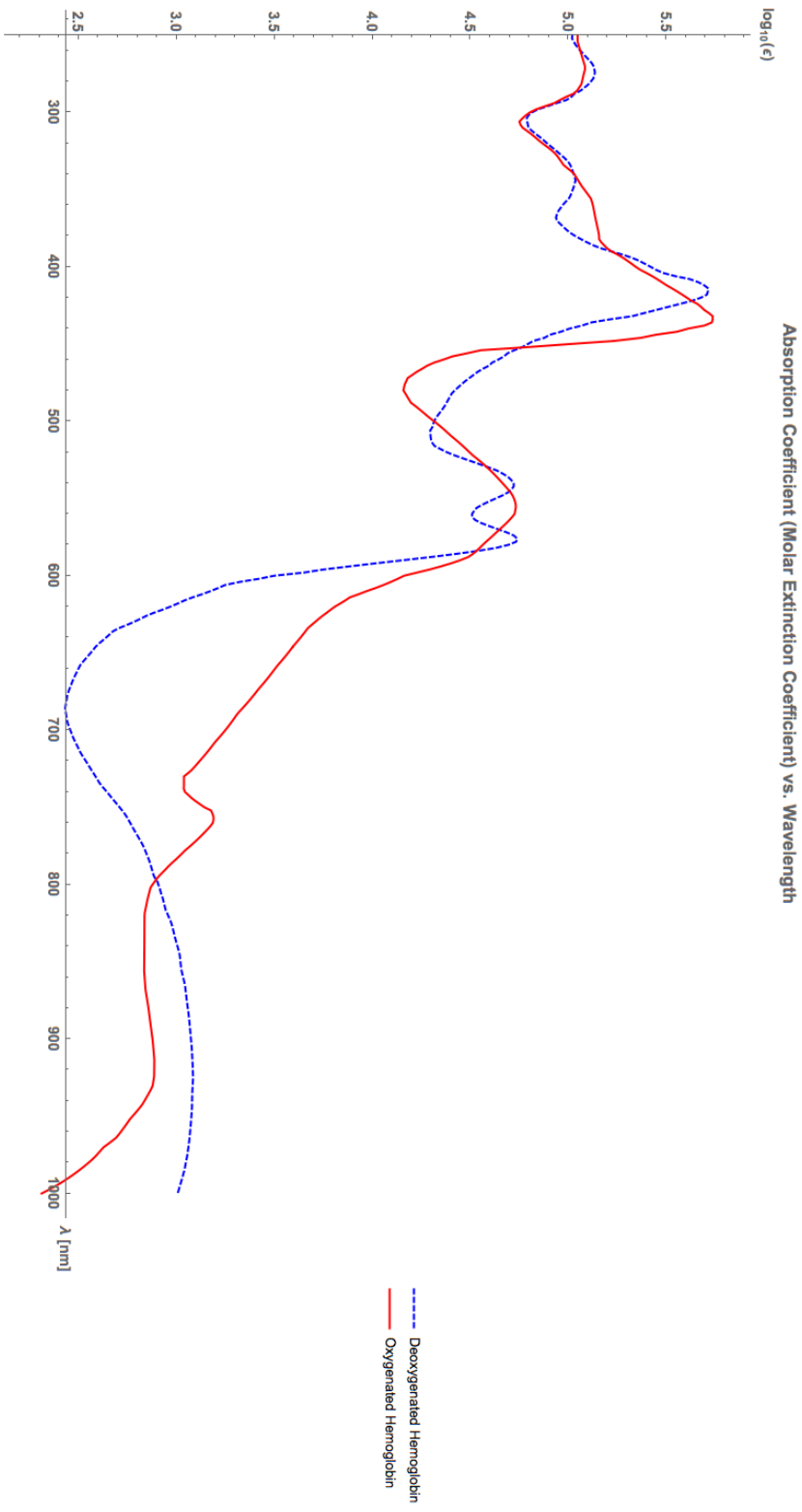

Figure 1- Molar Extinction Coefficient vs. Wavelength

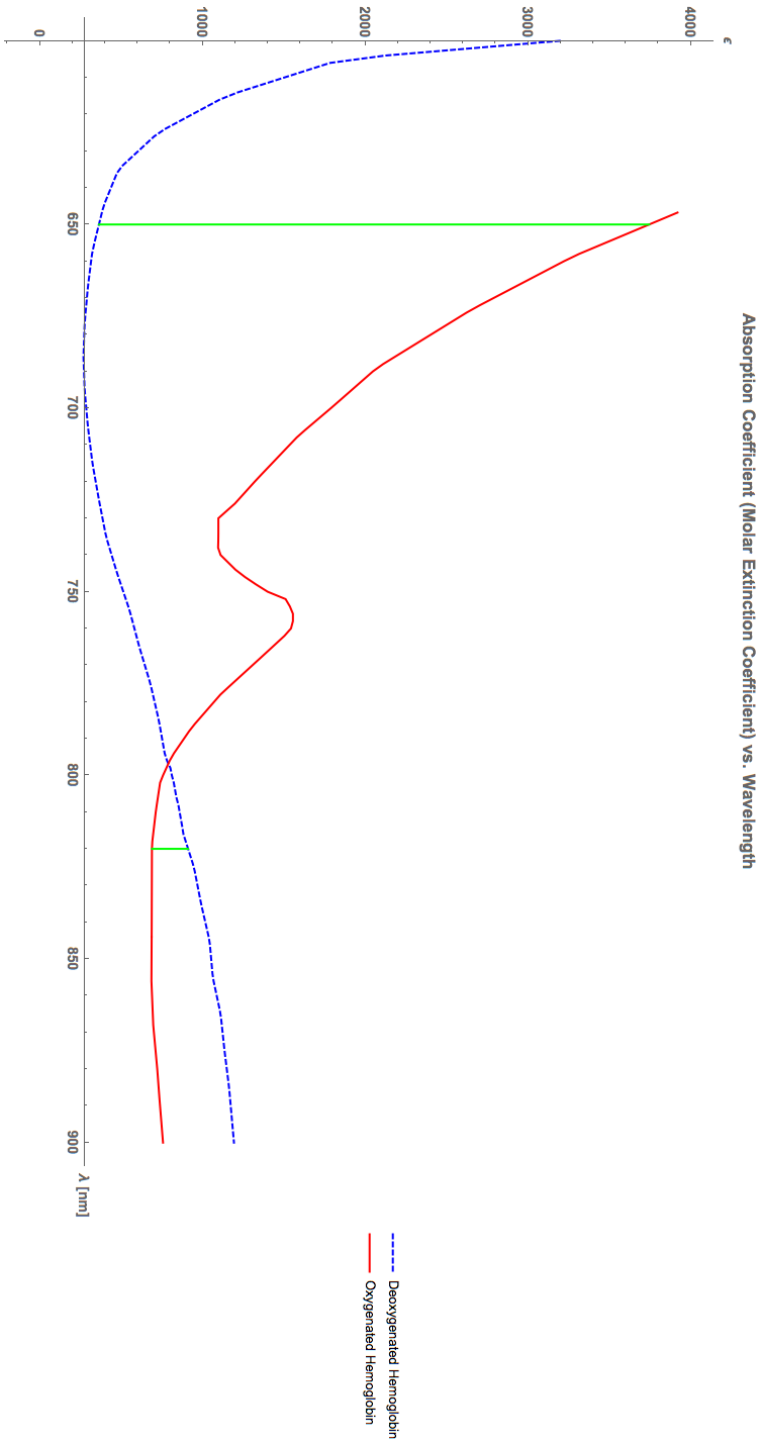

Figure 2 - Molar Extinction Coefficient vs. Wavelength (Appropriate scaling for experiment)

The system prototype was used to measure these differences in absorption is based on the principal of measuring the amplitude of the in-phase and quadrature components of the received optical signal. These amplitude measurements allow for the calculation of the absorption and path length of the test medium. Two notable points in the extinction coefficient plot are a point of larger difference in extinction coefficient at 650 nm and a point of smaller difference is near 820 nm. LEDs (and laser optics) are commonly available with these peak wavelengths. The absorption characteristics at the 820 nm wavelength are near the isosbestic point of absorption; a wavelength at which the absorption of oxygenated and deoxygenated hemoglobin are nearly identical. In the case of hemoglobin, the isosbestic point is used to calculate the concentration of hemoglobin, independent of oxygen concentration. At the isosbestic point, it should be assumed that the absorption of photons is in equal parts due to oxygenated and deoxygenated hemoglobin. Thus, the overall concentration of hemoglobin is solved for as follows:

$$c_T = c_{HbO_2} + c_{Hb} = 2\frac{\alpha(\lambda = 820nm)}{\ell_{820nm}\epsilon_{HbO_2}} = 2\frac{\alpha(\lambda = 820nm)}{\ell_{820nm}\epsilon_{Hb}} \quad (8)$$

Measurements Using In-Phase and Quadrature Demodulation

Phase delay, a value which is proportional to path length, can be calculated from measured parameters using an In-Phase and Quadrature (I-Q) receiver design. Phase delay can be calculated using the measured value of amplitude of the in-phase and quadrature components demodulated signal. This can be done, using a receiver using an analog to digital converter (ADC), which measures the DC voltage of baseband amplitude of the in-phase and quadrature components. Figure 3 shows an example block diagram for an I-Q measurement using an ADC.

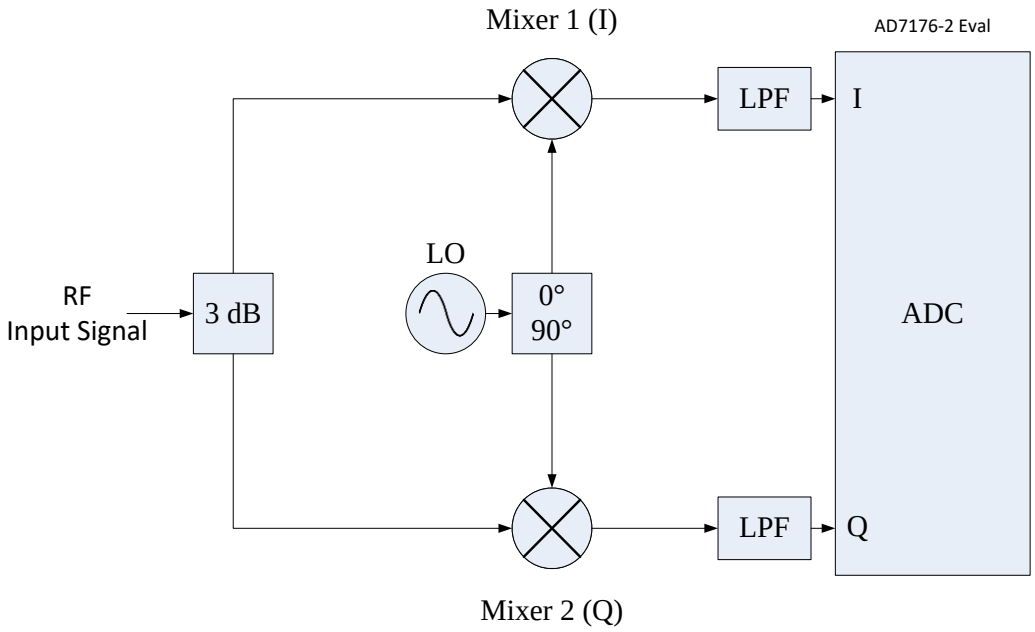

Figure 3 - I-Q Receiver Block Diagram

The optical signal is transmitted through the test medium and received by the photodiode. The test medium will induce a phase delay and power loss on the signal proportional to the concentration of the media present in the sample. The received signal is split (using an RF 3 dB signal splitter), and mixed with a local oscillator frequency of the same transmit frequency (homodyne) and the same local oscillator with a 90° phase shift. The demodulated signal is shown in Equation (9)

$$\cos\left(2\pi f_1 t+\phi_1\right)*\cos\left(2\pi f_{LO} t+\phi_{LO}\right)$$

$$=\frac{e^{j(2\pi f_1 t+\phi_1)}+e^{-j(2\pi f_1 t+\phi_1)}}{2}*\frac{e^{j(2\pi f_{LO} t+\phi_{LO})}+e^{-j(2\pi f_{LO} t+\phi_{LO})}}{2}$$

$$=\frac{e^{j(2\pi(f_1+f_{LO})+\phi_1+\phi_{LO})}+e^{-j(2\pi(f_1+f_{LO})+\phi_1+\phi_{LO})}}{2}$$

$$+\frac{e^{j(2\pi(f_1-f_{LO})+\phi_1-\phi_{LO})}+e^{-j(2\pi(f_1-f_{LO})+\phi_1-\phi_{LO})}}{2}$$

$$=cos(2\pi(f_1+f_{LO})+\phi_1+\phi_{LO})+cos(2\pi(f_1-f_{LO})+\phi_1-\phi_{LO}) \quad (9)$$

Where f_1 is the radio frequency (RF) input signal frequency and f_{LO} is the local oscillator (LO) frequency. Equation (9) are the terms at the intermediate frequency (IF) output port of each mixer. Each mixer will have a different ϕ_{LO} due to the 0-90° hybrid. The signal at the IF port of the mixers and before the low pass filter, the terms I and Q will be as follows

Mixer 1 IF Term=	Mixer 2 IF Term=
$\cos(2\pi(f_1+f_{LO})+\phi_1)+\cos(2\pi(f_1-f_{LO})+\phi_1)$	$\cos(2\pi(f_1+f_{LO})+\phi_1)+\cos(2\pi(f_1-f_{LO})+\phi_1-\frac{\pi}{2})$

When low pass filtered (LPF), the Mixer 1 and 2 IF terms are reduced to two terms I and Q; shown in Equations (10) and (11)

$$I=cos(2\pi(f_1-f_{LO})+\phi_1) \quad (10)$$

$$Q=cos(2\pi(f_1-f_{LO})+\phi_1-\frac{\pi}{2}) \quad (11)$$

The system is homodyne, thus f_1 has the same frequency f_{LO} such that the mixing of the signal and local oscillator result in a baseband term, which allows for even further simplification of I and Q, Equations (12) and (13)

$$I = cos(\phi_1) \tag{12}$$

$$Q = cos\left(\phi_1 - \frac{\pi}{2}\right) = sin(\phi_1) \tag{13}$$

It is possible to solve for the amplitude (A) and the phase delay (ϕ) using Equations (14) and (15) respectively, by measuring the DC voltages I and Q.

$$A = \sqrt{I^2 + Q^2} \tag{14}$$

$$\phi = tan^{-1}(\frac{Q}{I}) \tag{15}$$

The absorbance due to the medium under test, α, can be calculated using the following equation:

$$\alpha = log_{10}\left(\frac{A_B}{A_M}\right) \tag{16}$$

Where A_B is the baseline signal amplitude measured, found by measuring the I and Q voltages while the transmitter is directly connected to the receiver using a fiber optic cable and no medium. Measured as such, the baseline signal amplitude would be accounting of measurement system losses. A_M represents the amplitude of the signal when a medium is present, which also includes the baseline absorption. The absorption of the medium alone is then calculated based on the difference between the baseline amplitude and the amplitude with the medium present.

The path length can be estimated from the phase delay using equation (17) where λ_e is the electrical (modulation) wavelength and ℓ is the optical path length difference.

$$\ell = \frac{\phi}{2\pi} * \lambda_e \tag{17}$$

Chapter II: Design and Implementation

The system used to prototype this design is named the Blood Oxygenation LED Tomography (BOLT). BOLT consists of modular components; each can be changed to modify design parameters. The system consists of a transmitter, receiver and a PC, which is used for control and data acquisition. Figure 4 shows the overall system block diagram.

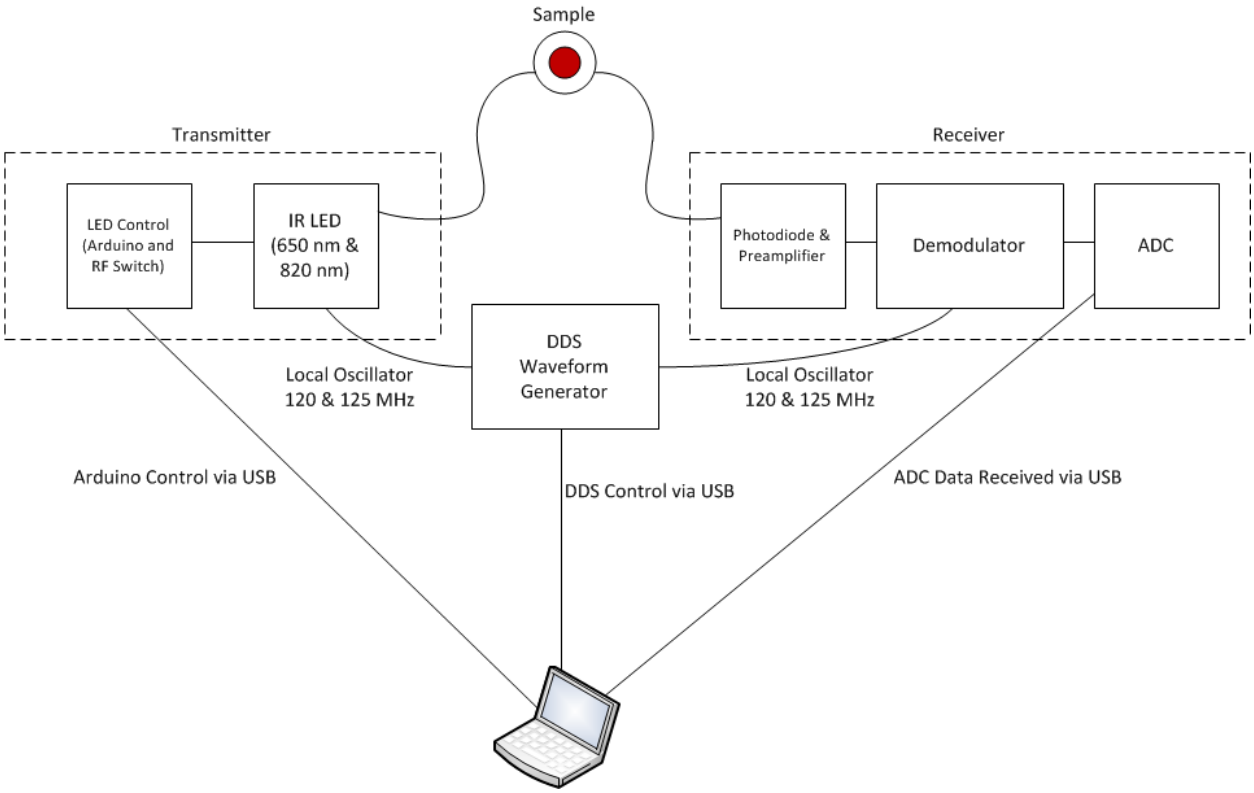

Figure 4 - System Block Diagram

A PC is connected to an Arduino, the DDS waveform generator, and the ADC via USB. The PC provides the following functions in the system:

- Arduino Control – The Arduino is programmed by the PC to set 4 digital output signals to control channel selection of the RF switch on the transmitter board. The RF switch selects

which LED is active in the system. The RF switch has 2 simultaneous channels, one used for the selection of the 650 nm LED and 820 nm LED.

- The Analog Devices AD9958 Direct Digital Synthesis Evaluation Board (DDS) is responsible for generating the 120 MHz and 125 MHz sinusoidal signals used for the intensity modulation of the LEDs and the local oscillator signal of the demodulation board. The PC provides control of the output frequency and phase shift of the DDS.
- The Analog Devices EVAL-AD7176-2SDZ Analog-to-digital Converter (ADC) is used to measure the DC voltage at the output of the system receiver (BOLT-DEMOD). The measurements that the ADC collects is captured and stored using the PC.

Receiver – Photodiode and Pre-amplifier (BOLT-PD)

The receiver is divided into modular circuit boards such that, for future designs, different components can be modified, such as photodiodes or optical to electrical converters. The first modular board, BOLT-PD, includes a photodiode, pre-amplifier and band pass filter. It was anticipated that a wide range of signal loss would be introduced with a sample medium, so the pre-amplifier was designed to provide signal gain. Amplifier designs with large amounts of gain are susceptible to parasitic oscillation. Parasitic oscillation occurs when the output stage of the amplifier couples into the input, thus creating a positive feedback loop. This feedback noise can become powerful enough to reduce the signal to noise ratio of the received signal. Parasitic oscillations are also often referred to as "ringing." To reduce interference from outside sources and to reduce amplifier ringing, a band pass filter, only passing frequencies from 110 to 140 MHz, was included as part of the BOLT-PD. Figure 5 shows a high-level block diagram of the BOLT-PD. A complete schematic and board layout are shown in Appendix A.

Figure 5 - BOLT-PD Block Diagram

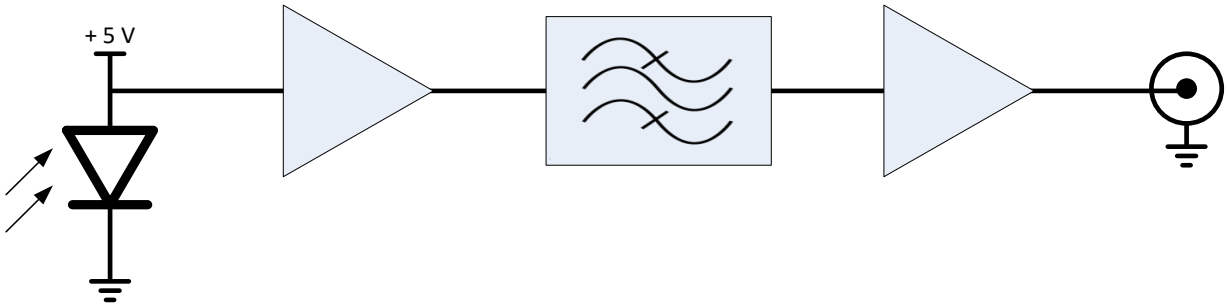
+ 5 V

Receiver – Demodulator (BOLT-Demod)

The optical signal is amplified and band-pass filtered by BOLT-PD. The signal from the output of BOLT-PD is input to the demodulator circuit board, named BOLT-Demod. BOLT-Demod is a receiver designed to frequency shift modulated signal components to baseband such that an analog-to-digital converter can sample measurements at less than 10 Hz. The schematic and PCB layout of the BOLT-PD and BOLT-Demod board are shown in Appendix B.

The basic purpose of the DDS is to generate 120 MHz and 125 MHz sinusoidal signals. Each signal is input to a 0°/90° hybrid splitter. The hybrid splitter performs the same function as a normal 3 dB splitter except that the first output of the splitter has no phase shift and the second output of the hybrid has been shifted by 90° of relative phase shift. The output of two hybrid splitters, one at each frequency, 120 MHz and 125 MHz, produce the following signals:

1. 120 MHz with 0° relative phase shift
2. 120 MHz with 90° relative phase shift
3. 125 MHz with 0° relative phase shift
4. 125 MHz with 90° relative phase shift

The above signals generated by the DDS and hybrid splitters, are the local oscillator signals of four separate RF mixers. This mixing results in four Intermediate Frequency (IF) signals at baseband or DC voltages respectively:

1. Amplitude of the in-phase component at 120 MHz (I_{120})
2. Amplitude of the quadrature component at 120 MHz (Q_{120})
3. Amplitude of the in-phase component at 125 MHz (I_{125})
4. Amplitude of the quadrature component at 125 MHz (Q_{125})

The IF output of the mixer is low pass filtered to minimize any higher order signal terms. This design uses a 3-pole passive RC low pass filter. The amplitude of the filtered IF output of the mixers is measured using an analog-to-digital converter (ADC) which has 4 inputs, one for each I and Q output voltage.

Receiver – Analog to Digital Converter (ADC)

It is necessary to design a receiver which has low ADC quantization noise such that the signal to noise ratio (SNR) is maximized. In order for the received signal to be detectable it must have more power than the ADC quantization noise. The ADC is limited to a minimum amount signal power that it is able to detect. This limit is determined by the number of bits of resolution the ADC has, as well as the range of voltage it can detect. The quantization noise power P_{QN} is calculated from the quantization noise voltage V_{QN} found using equation (18). The quantization noise voltage is proportional to the voltage range that the ADC is capable of measuring divided by the number of possible values the ADC can produce. The quantization noise power can be calculated using equation (19) where R is equivalent resistance at the input of the ADC. In the case of a measurement made at the output of an RF mixer, the resistance seen by the ADC is 50 Ω. Equation (20) shows the conversion to units of dBm.

$$V_{QN} = \frac{V_{range}}{2^B} \text{ [V]} \tag{18}$$

$$P_{QN} = \frac{{V_{QN}}^2}{R} \ [W] \tag{19}$$

$$P_{QN}[dBm] = 10 * log_{10}(P_{QN}/1\,mW) \tag{20}$$

The ADC selected for this design has a voltage range of 2.5 V to -2.5 V and 24 bits of resolution. Thus the calculated quantization noise floor of this ADC is approximately -117 dBm. The quantization noise floor was calculated as follows:

$$V_{QN} = \frac{V_{Range}}{2^B} = \frac{5}{2^{24}} \approx 0.29\ \mu V \tag{21}$$

$$P_{QN} = \frac{{V_{QN}}^2}{R} = \frac{(0.29\mu V)^2}{50\Omega} \approx 1.78\ fW \tag{22}$$

$$P_{QN}[dBm] = 10 * log_{10}\left(\frac{1.78fW}{1mW}\right) \approx -117.5\ dBm \tag{23}$$

Essentially, this value represents the minimum power detectable by the ADC. Any signals with less power than -117.5 dBm will not be measured by the ADC and thus considered to be below the quantization noise floor.

Transmitter

The basic purpose of the infrared transmitter (further referred to as IR Tx or Tx) is to provide two optical sources of 650 nm and 820 nm, which are intensity modulated (IM) at two different electrical frequencies of 120 MHz and 125 MHz respectively. Assigning the two wavelengths to separate electrical modulation frequencies provides a method to differentiate between the two signals upon detection, thus allowing for measurements of absorption and path length independently for each wavelength. Intensity modulation can be achieved through the use of a simple current drive circuit using a BJT and RF amplifier.

Chapter III: Experimental Results

Simulated Tissue Experiment (Blood phantom)

India ink has similar spectral absorption properties to hemoglobin, specifically in the spectral range of 650 and 820 nm wavelengths and is commonly used as a substitute for hemoglobin in near-infrared spectrum measurements. Thus a water and India ink solution is used to simulate blood and is referred to as "blood phantom". As demonstration of the transmitter and receiver design concept, tests were performed using water and also using a blood phantom. Tests were performed by submerging transmit and receive fiber optic cables inside a sample container (glass) holding water to simulate a sample containing no blood as baseline for proof of concept. Similarly, to study the effect of optical attenuation, the fiber optic cables were spaced from 0 cm to 5 cm apart, varying by 1 cm each test. During each test, the ADC was used to sample the I and Q DC voltage approximately 1000 times at a rate of 5 samples per second (5 Hz) for a total duration of approximately 200 seconds. Figure 6 below shows a diagram of the test apparatus used to perform the experiment.

Figure 6 - Water and Ink Experiment Diagram

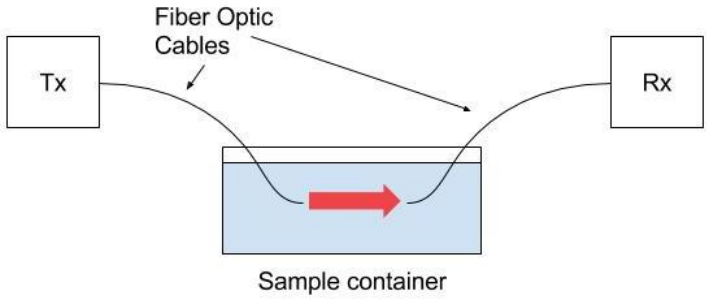

During test cases using blood phantom, a single 820 nm LED was enabled in order to simplify testing. The ADC measured the I and Q voltages from the 120 MHz receiver (electrical frequency

assigned to the 650 nm LED). It should be noted that the technique used to determine the baseline signal amplitude (A_B) involved using a short length of fiber optic cable with ST-connector terminations on each end of the cable. The cable was then connected directly between the transmitter and receiver; however, this did not represent the actual experimental setup and the baseline measurements were not useable. As such, the baseline signal amplitude values used in Equation 16 were estimated by linear extrapolation back to 0 cm using the signal amplitude measurements at 1 cm and 2 cm separation for the water measurements. This was based on the thinking that the water sample represented the lowest absorption of light and, therefore, the extrapolation would result in a closer approximation of the system losses. Figure 7, below, shows the calculated phase angle via Equation (15) based on the measured I and Q voltages for experiments involving water (shown blue) and water with ink (shown red). The difference in calculated phase angle, using 820 nm light, is less than 1° indicating that the phantom blood sample and the water sample have approximately the same optical path length difference at 820 nm. This demonstrates that the blood phantom and water simulate the 820 nm isosbestic light absorption characteristic of hemoglobin as was expected.

Figure 7 - Calculated Phase Difference at 820 nm (Isosbestic Point)

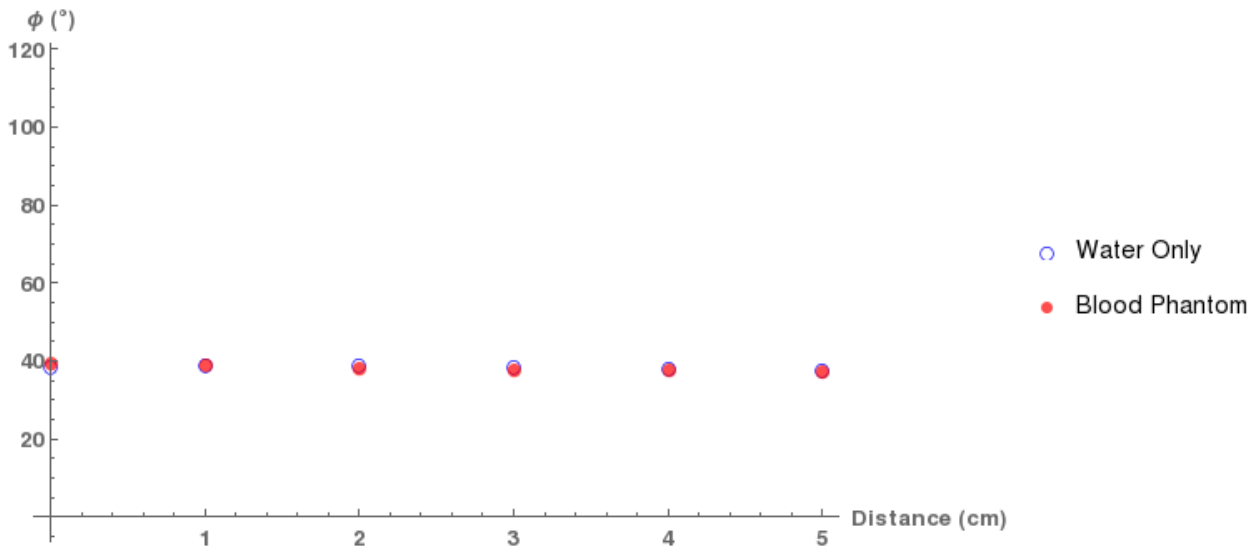
ϕ (°)
120
100
80
60
40
20
1
2
3
4
5
Distance (cm)
Water Only
Blood Phantom

The experiment was repeated, instead, enabling a single 650 nm LED. Figure 8, below, shows the calculated phase angle at 650 nm. In this plot, the phase angle of the blood phantom sample is greater than that of the water sample (approximately 39° on average) which is an indication that optical path length difference of light at 650 nm increases with increasing ink concentration. This demonstrates that the blood phantom simulated the selective absorption characteristic of hemoglobin as was expected.

Figure 8 - Calculated Phase Difference at 650 nm

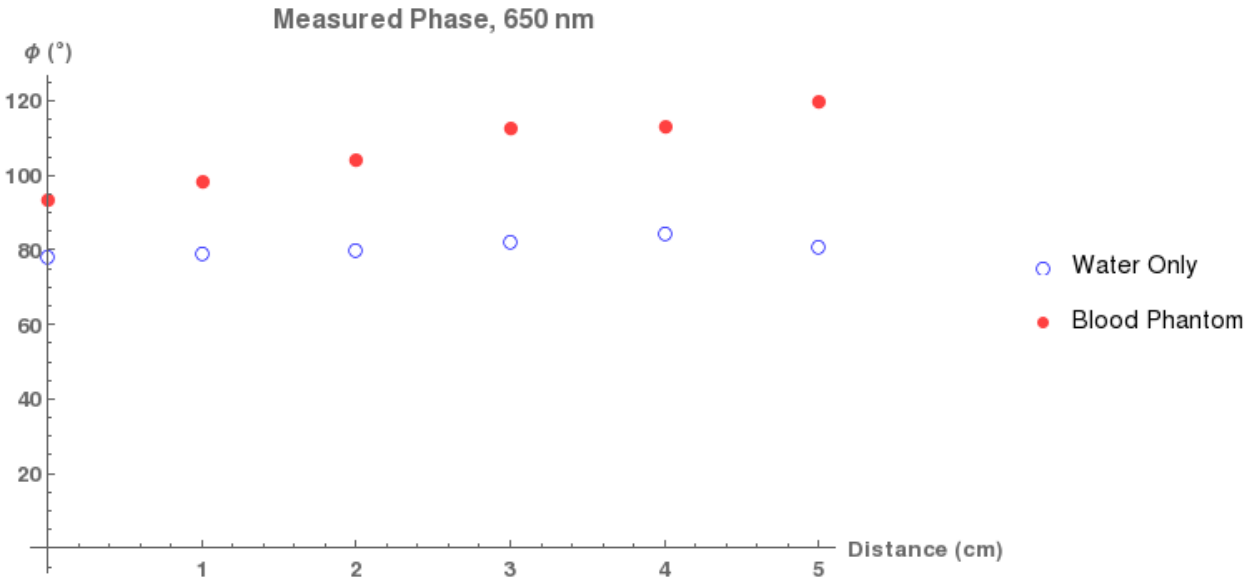

As demonstrated by the data gathered and shown in Figure 7 and Figure 8, the system is able to resolve a difference in phase angle when measuring using the 650 nm wavelength LEDs and the near-zero difference in phase angle when measuring using the 820 nm wavelength LEDs. Data from these plots can be used to solve for the concentration of deoxygenated and oxygenated hemoglobin in the sample using Equations (6) and (7).

Figure 9 and Figure 10 show the calculated amplitude (Equation 14) from the received I and Q signals at 820 nm and 650 nm respectively which later leads to the calculation of signal attenuation. Figure 9 demonstrates an isosbestic behavior of the blood phantom at 820 nm in that there is a small difference in calculated amplitude between pure water and the water-india-ink mixture. This is due to there being little difference in absorption of 820 nm wavelength light in the water sample and in water-india-ink sample. Figure 10 demonstrates a non-isosbestic behavior of the blood phantom when measuring with 650 nm wavelength light as seen in the large difference in calculated amplitude between pure water and the water-india-ink mixture. Figure 10 also demonstrates higher absorption of 650 nm wavelength light in the water-india-ink mixture.

Figure 9 - Calculated Amplitude at 820 nm (Isosbestic Point)

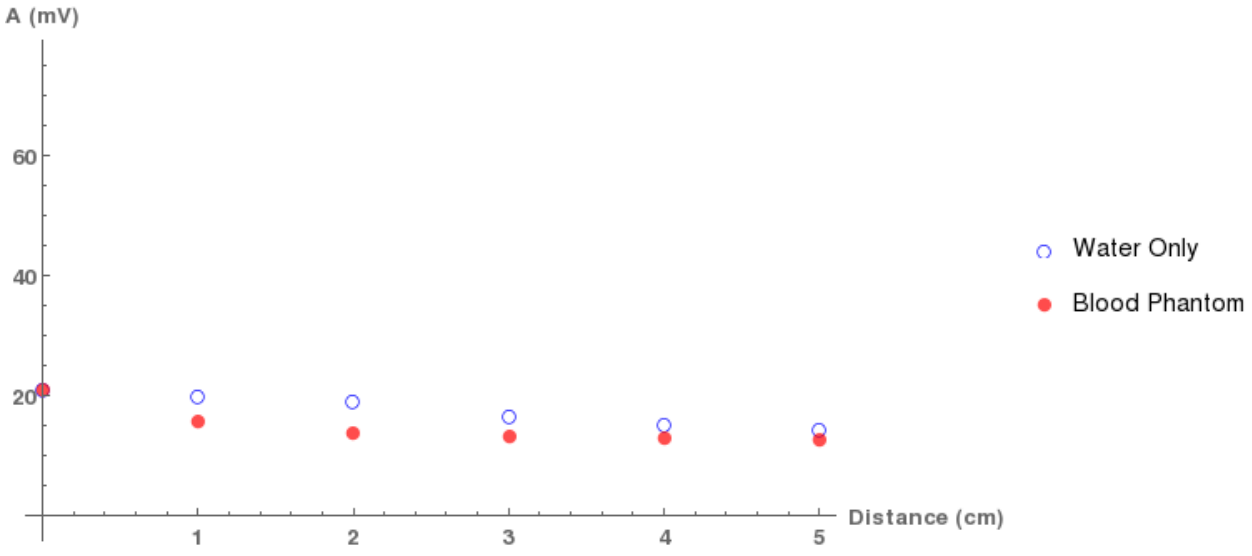

Figure 10 - Calculated Amplitude at 650 nm

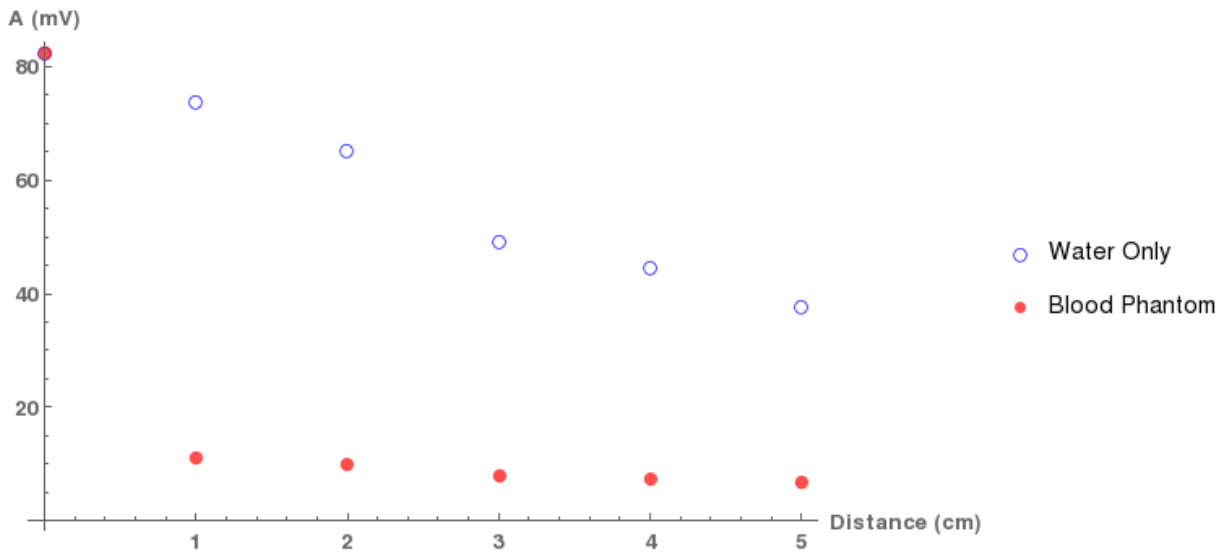
A (mV)
80
60
40
20
1
2
3
4
5
Distance (cm)
Water Only
Blood Phantom

Figure 11 and Figure 12 show the calculated absorbance (Equation 16) of the received signal at 820 nm and 650 nm based on the amplitude results of Figures 9 and 10 respectively. The baseline signal amplitudes, A_B, used in Equation 16, are those values of signal amplitudes shown in Figures 9 and 10 at zero centimeter optic cable spacing.

Figure 11 - Calculated Absorbance at 820 nm (Isosbestic Point)

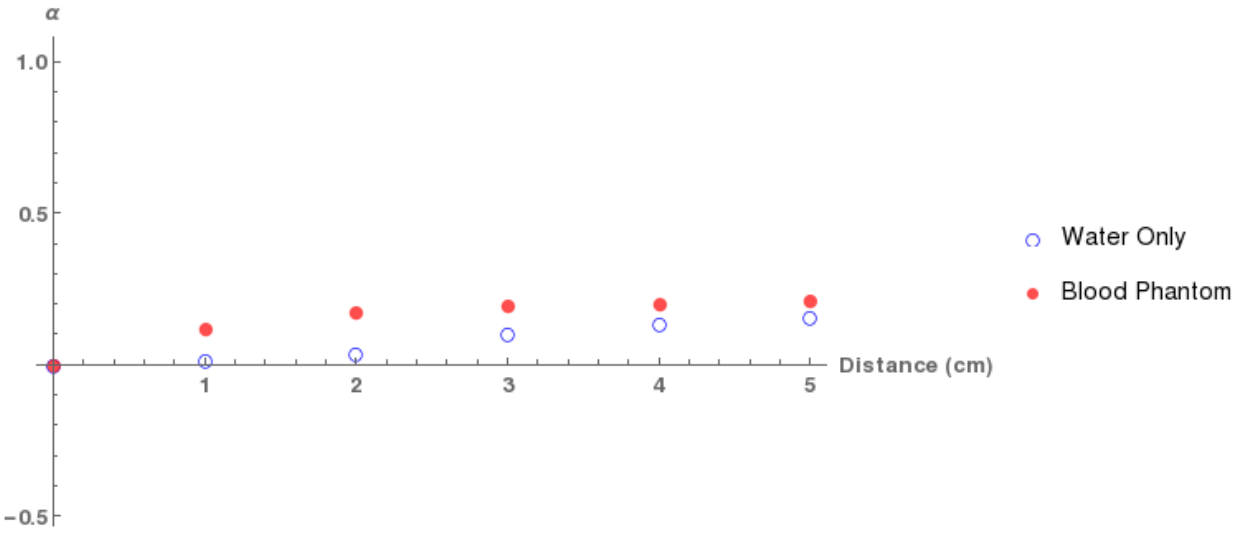

Figure 12 - Calculated Absorbance at 650 nm

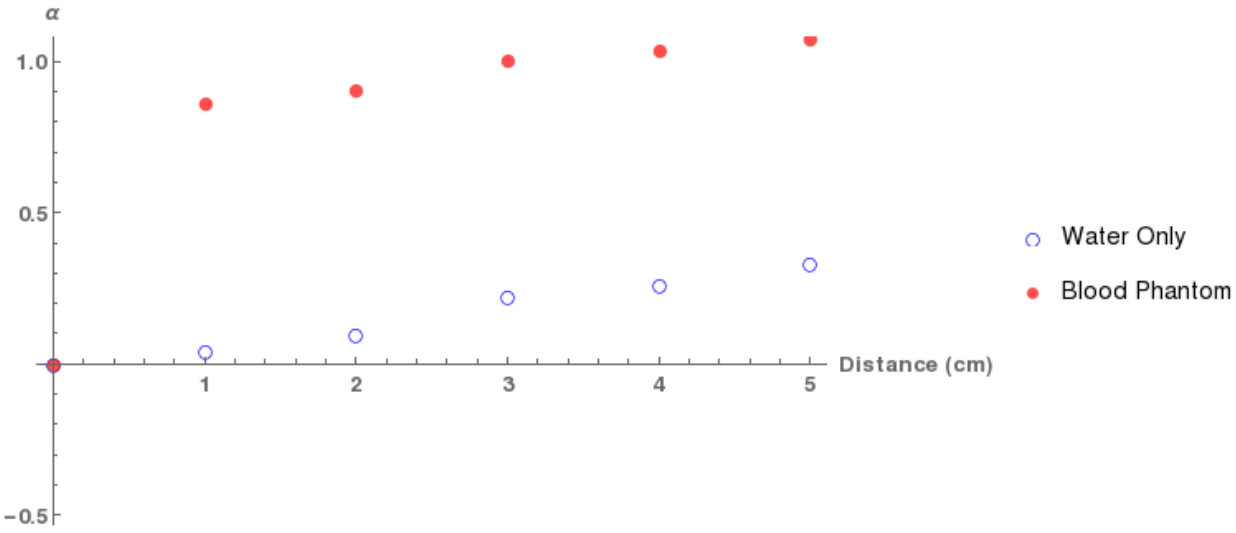

Figure 13 and Figure 14 show the calculated path length difference (Equation 17) from 820 nm and 650 nm measurements respectively. Path length difference is directly proportional to phase and modulation wavelength according to Equation 17. As a result Figures 13 and 14 are simply scaled versions of Figures 7 and 8.

Figure 13 - Calculated Path Length Difference at 820 nm (Isosbestic Point)

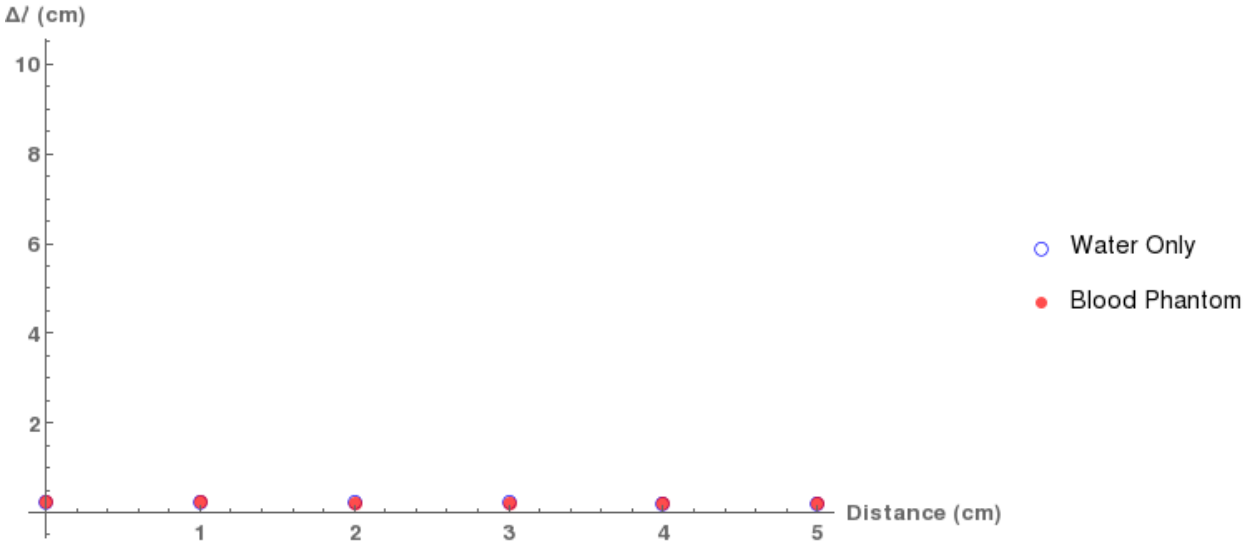

Figure 14 - Calculated Path Length Difference at 650 nm

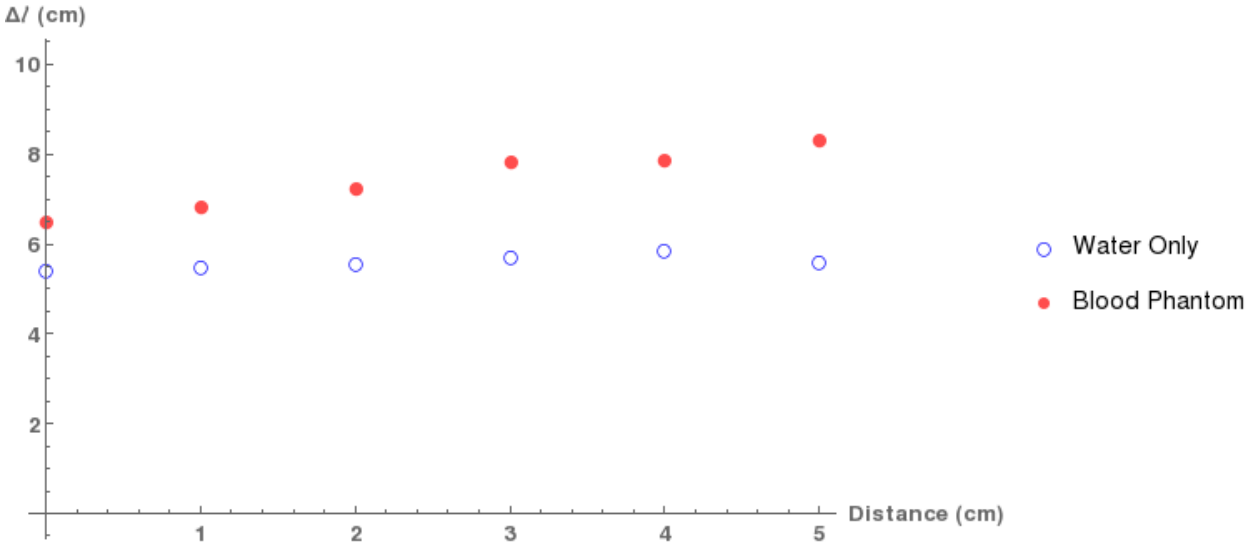

Finally Figure 15 and Figure 16 show the calculated deoxygenated and oxygenated hemoglobin concentrations (Equation 16) respectively for the water sample and the blood phantom sample. Both Figure 15 and 16 are showing an increasing measurement of deoxygenated and oxygenated hemoglobin concentrations in the water sample, indicating an increasing error in measurement with increasing fiber optic separations. Figure 15 shows that the measurement of deoxygenated hemoglobin concentration in the blood phantom sample remains relatively constant with increasing fiber optic separation. However, Figure 16 shows that an increasing error in the measurement of oxygenated hemoglobin in the blood phantom sample with increasing fiber optic separation.

Figure 15 - Calculated Concentration of Deoxygenated Hemoglobin

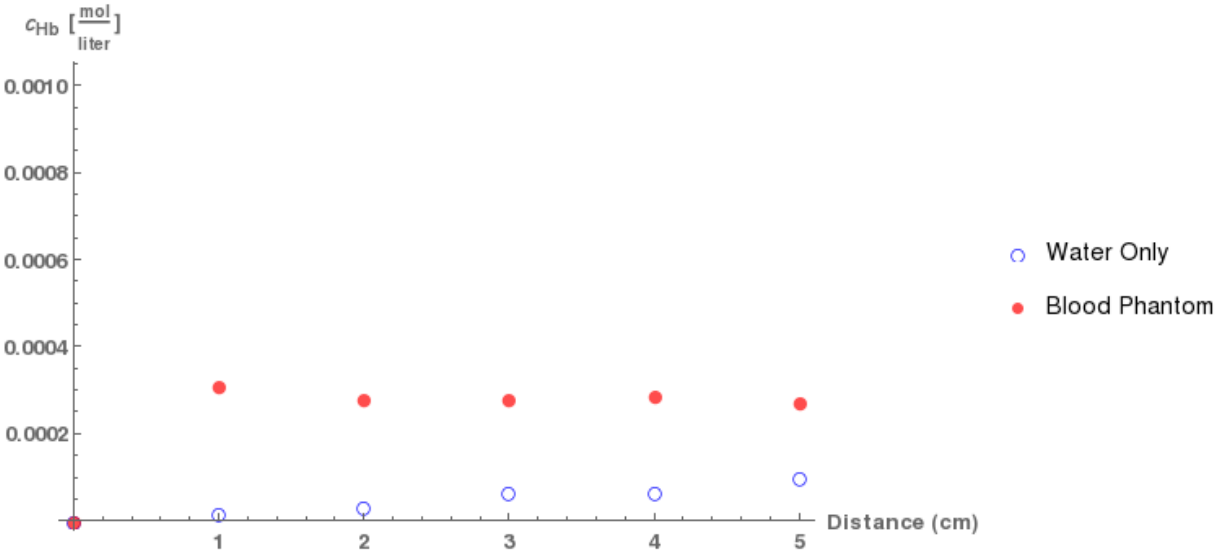

Figure 16 - Calculated Concentration of Oxygenated Hemoglobin

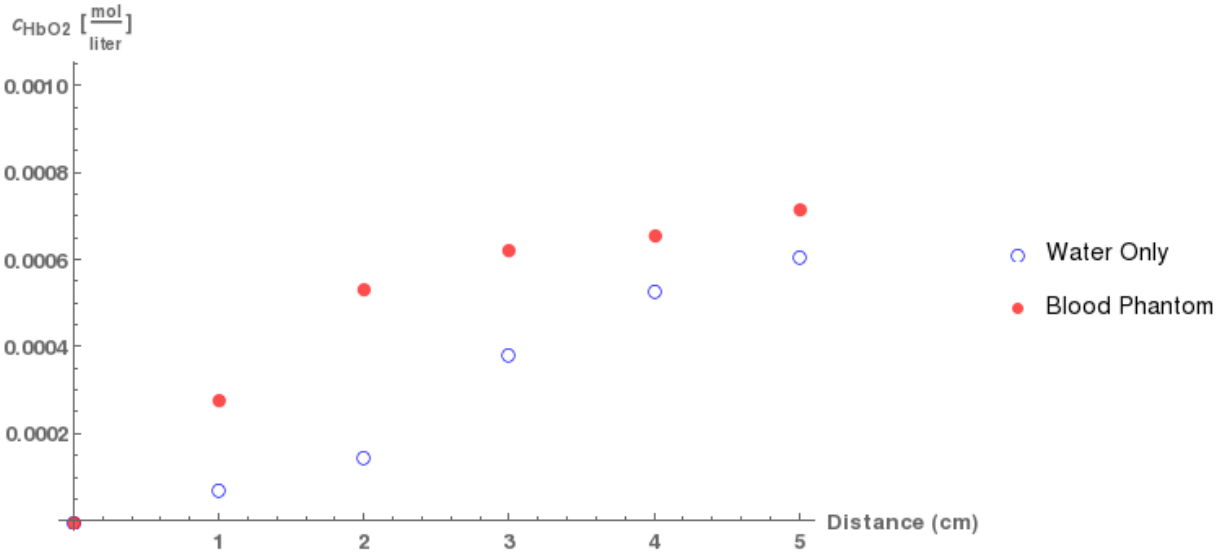
c_{HbO2} [$\frac{mol}{liter}$]
0.0010
0.0008
0.0006
0.0004
0.0002
1
2
3
4
5
Distance (cm)
Water Only
Blood Phantom

Chapter IV: Uncertainty Analysis

This section presents an uncertainty analysis of the blood concentration calculations, presented above, based on the uncertainty of the I and Q measurements.

The uncertainty each I and Q measurement can be evaluated as follows:

$$U_{meas} = \sqrt{{S_1}^2 + {S_2}^2} \tag{24}$$

$$S_1 = \frac{\sigma_{meas}\, F}{\sqrt{n_{meas}}} \tag{25}$$

$$S_2 = \frac{\sqrt{R_{inst}}}{\sqrt{3}} \tag{26}$$

Where;

U_{meas} is the uncertainty of the measurement.

σ_{meas} is the standard deviation of the samples of the measurement.

F is a factor based on the Student's T distribution. F is 1 if more than 30 samples are taken.

n_{meas} is the number samples of the measurement.

R_{inst} is the instrument resolution, also known as V_{QN} = 0.29 µV based on Equation (21)

Referring to Equations (6) and (7), the uncertainty of the concentration calculations can be determined as follows:

$$\left(U_{C_{Hb}}\right)^2 = \left(\frac{\partial C_{Hb}}{\partial Q_{650}}\right)^2 \left(U_{Q_{650}}\right)^2 + \left(\frac{\partial C_{Hb}}{\partial Q_{820}}\right)^2 \left(U_{Q_{820}}\right)^2 + \left(\frac{\partial C_{Hb}}{\partial I_{650}}\right)^2 \left(U_{I_{650}}\right)^2 + \left(\frac{\partial C_{Hb}}{\partial I_{820}}\right)^2 \left(U_{I_{820}}\right)^2 \quad (27)$$

$$\left(U_{C_{HbO_2}}\right)^2 = \left(\frac{\partial C_{HbO_2}}{\partial Q_{650}}\right)^2 \left(U_{Q_{650}}\right)^2 + \left(\frac{\partial C_{HbO_2}}{\partial Q_{820}}\right)^2 \left(U_{Q_{820}}\right)^2 + \left(\frac{\partial C_{HbO_2}}{\partial I_{650}}\right)^2 \left(U_{I_{650}}\right)^2 + \left(\frac{\partial C_{HbO_2}}{\partial I_{820}}\right)^2 \left(U_{I_{820}}\right)^2 \quad (28)$$

Where:

U_{I_λ} is the measurement uncertainty of I for λ wavelength light.

U_{Q_λ} is the measurement uncertainty of Q for λ wavelength light.

Table 2 presents the results of the above described uncertainty analysis applied to measurements of the water and blood phantom samples.

Table 2 - Calculated Uncertainty

	d=1 cm	d=2 cm	d=3 cm	d=4 cm	d=5 cm
U(c_{Hb} of water)	3.14536×10^{-6}	3.32722×10^{-6}	4.1221×10^{-6}	4.6898×10^{-6}	5.25722×10^{-6}
U(c_{HbO2} of water)	30.4998×10^{-6}	32.0386×10^{-6}	39.2453×10^{-6}	44.8723×10^{-6}	49.17×10^{-6}
U(c_{Hb} of water and ink)	11.4758×10^{-6}	14.7747×10^{-6}	23.8499×10^{-6}	26.6747×10^{-6}	35.642×10^{-6}
U(c_{HbO2} of water and ink)	42.4851×10^{-6}	52.9793×10^{-6}	59.1335×10^{-6}	61.785×10^{-6}	67.0103×10^{-6}

Based on Table 2, the greatest uncertainty value, $67x10^{-6}$, is the concentration of oxygenated hemoglobin measured at a fiber separation distance of 5 cm. Therefore, the level of uncertainty of the calculated concentrations is low due to the high level of accuracy of the ADC.

Chapter V: Conclusions

The purpose of the work presented in this paper was to develop a proof-of-concept prototype device which implements an In-phase and Quadrature receiver design to measure the phase shift and amplitude attenuation of near infrared light. These measurements are used for determination of path length difference and absorbance for use in the Beer-Lambert Law in calculation of oxygenated and deoxygenated blood concentrations. The prototype system was capable of resolving phase difference and amplitude attenuation in measurements using water and blood phantom samples. Data from these measurements was used in example calculation of concentration of oxygenated versus deoxygenated hemoglobin of the simulated medium. The system appears to demonstrate an increasing error in concentration measurements with increasing fiber optic separation distance. This is likely due to the decrease of signal-to-noise ratio of the electrical signal output from the photodiode due to the addition of relatively constant amplitude noise form the photo diode to an ever decreasing amplitude of the light signal measured by the photodiode. Increased light source intensity would act to increase signal-to-noise ratio at the larger fiber optic separations. This would require an LED transmitter with greater power output and/or a photodiode receiver with greater sensitivity. In addition, a reduction in noise introduced at the photodiode could be accomplished by improving the system electromagnetic interference shielding. The system was demonstrated with 650 nm and 820 nm light sources being active separately. Further experimentation will be needed with both light sources active at the same time to demonstrate use in a practical application.

An experiment was performed with a human finger in place of the blood phantom to determine if blood oxygen concentration could be measured in vivo. The result of that experiment was that no signal was detected due to losses. Therefore, the system signal to noise ratio would need to be increased by increasing light source intensity.

Future applications could include the modification of the BOLT-PD section of the system to improve upon photodiode receiver sensitivity and LED transmitter output power and amplitude modulation frequency range. Future improvements could involve replacing the transmitting LED with an electrically modulated coherent light source such as a laser to further improve signal-to-noise ratio. The system would use homodyne coherent mixing, to perform signal demodulation at optical frequencies. The system must also include an I-Q splitter (i.e., hybrid splitter) in order to resolve I and Q amplitudes. To measure phase difference, the laser would need to be electrically amplitude modulated, otherwise the optical path length difference would be 0 to 650 nm or 0 to 820 nm which is not sufficient for samples much greater than 650 or 820 nm in optical distance such as a human head.

References

[1] V. O. Rybynok and P. A. Kyriacou, "Beer-lambert law along non-linear mean light pathways for the rational analysis of Photoplethysmography," *Journal of Physics: Conference Series*, vol. 238, no. 012061, pp. 1-6, 2010.

[2] A. Pellicer and M. del Carmen Bravo, "Near-infrared spectroscopy: A methodology-focused review," *Seminars in Fetal & Neonatal Medicine*, vol. 16, no. 1, pp. 42-49, 2011.

[3] S. E. LeBlanc, M. Atanya, K. Burns and R. Munger, "Quantitative impact of small angle forward scatter on whole blood oximetry using a Beer–Lambert absorbance model," *Analyst*, vol. 136, p. 1637–1643, 2011.

[4] D. B. MacLeod and et al, "Development and Validation of a Cerebral Oximeter Capable of Absolute Accuracy," *Journal of Cardiothoracic and Vascular Anesthesia*, vol. 26, no. 6, pp. 1007-1014, 2012.

[5] Y. Yang, E. Gussakovsky, J. Rendell, O. Jilkina and V. Kupriyanov, "Mapping the myoglobin concentration, oxygenation, and optical pathlength in heart ex vivo using near-infrared imaging," *Analytical Biochemistry*, vol. 407, pp. 120-127, 2010.

[6] G. Strangman, M. A. Franceschini and D. A. Boas, "Factors affecting the accuracy of near-infrared spectroscopy concentration calculations for focal changes in oxygenation parameters," *NeuroImage*, vol. 18, p. 865–879, 2003.

[7] A. Vermeij, A. H. E. A. van Beek, M. G. M. Olde Rikkert and J. A. H. R. Claassen, "Effects of Aging on Cerebral Oxygenation during Working-Memory Performance: A Functional Near- Infrared Spectroscopy Study," *PLOS ONE*, vol. 7, no. 9, pp. 1-11, 2012.

[8] S. Prahl, "Optical Absorption of Hemoglobin," 15 Dec 1999. [Online]. Available: http://omlc.ogi.edu/spectra/hemoglobin/index.html. [Accessed August 2013].

[9] *IUPAC. Compendium of Chemical Terminology, 2nd ed. (the "Gold Book"). Compiled by A. D. McNaught and A. Wilkinson. Blackwell Scientific Publications, Oxford (1997). XML online corrected version: http://goldbook.iupac.org (2006-) created by M. Nic, J. Jir.*

Appendix A – Schematics

Appendix A.1.1 – BOLT-Tx Schematic (RF Switch and Connectors)

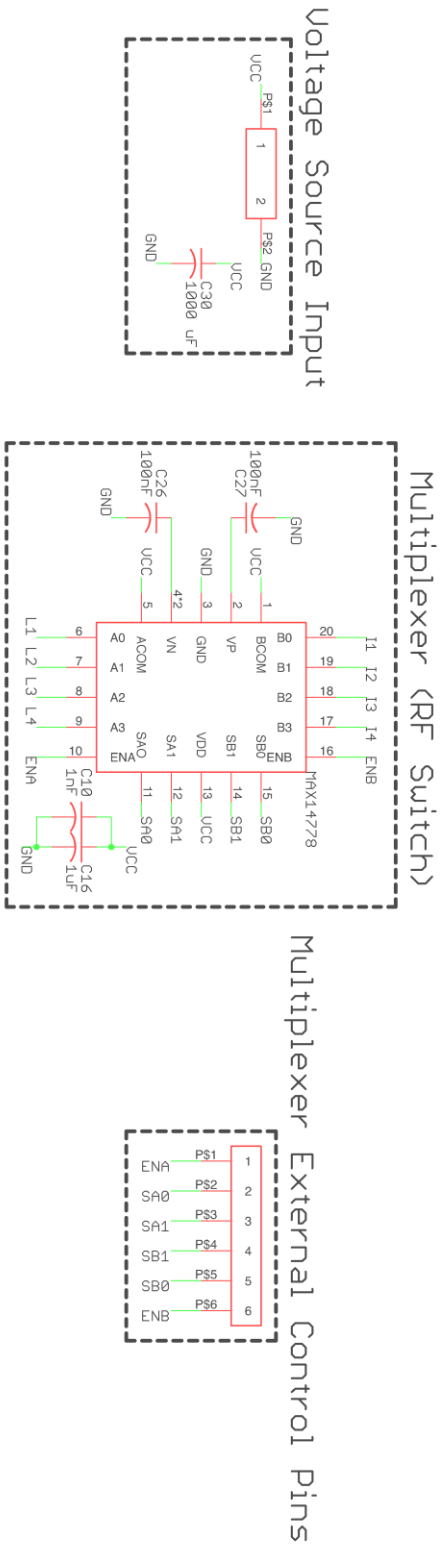

Appendix A.1.2 – BOLT-Tx Schematic (650 nm LEDs and RF Choke

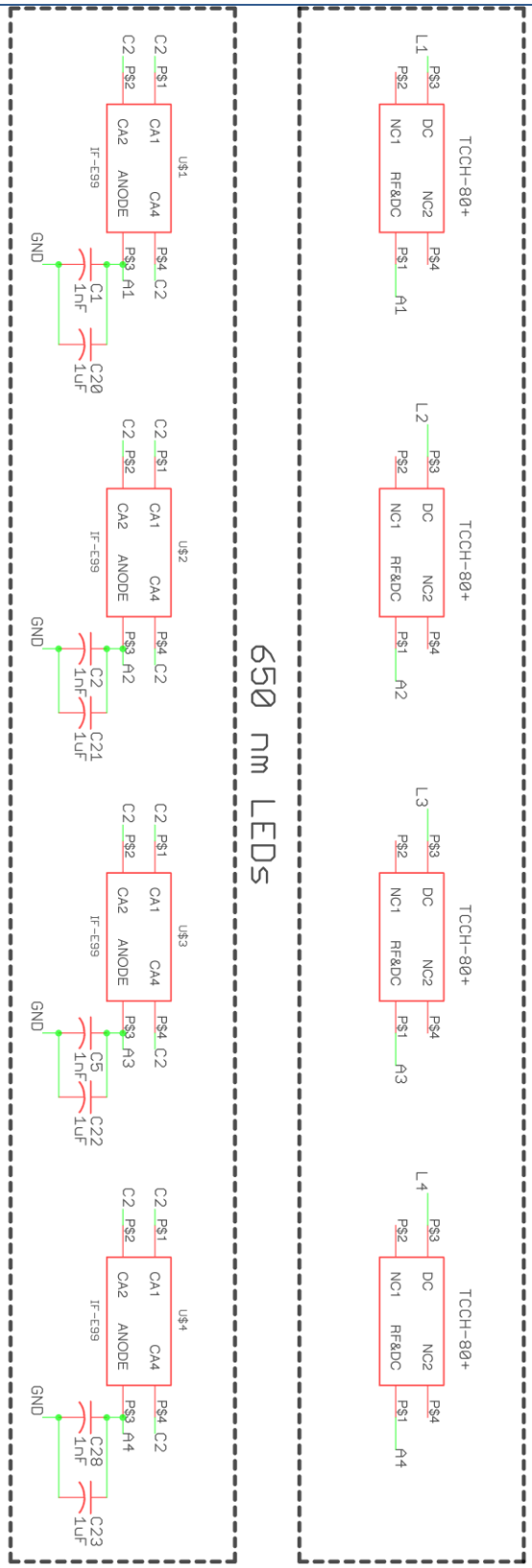

Appendix A.1.3 – BOLT-Tx Schematic (820 nm LEDs and RF Chokes)

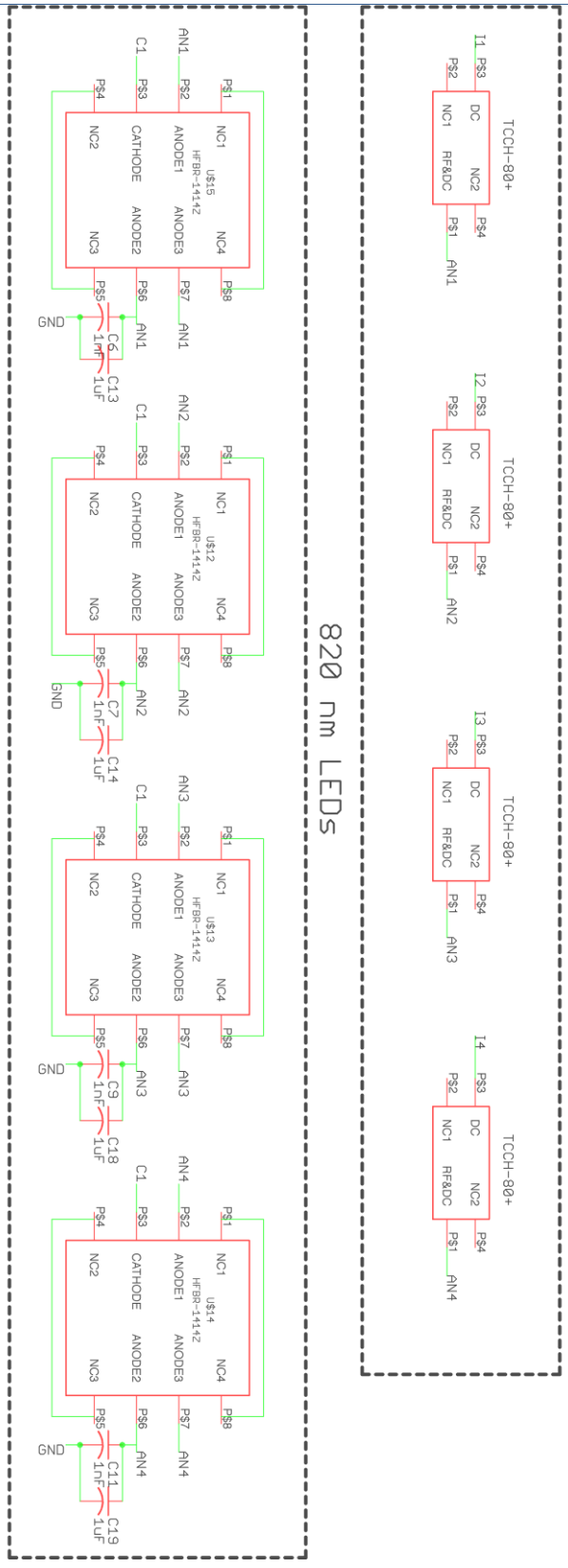

Appendix A.1.4 – BOLT-Tx Schematic (650 nm LED Driver)

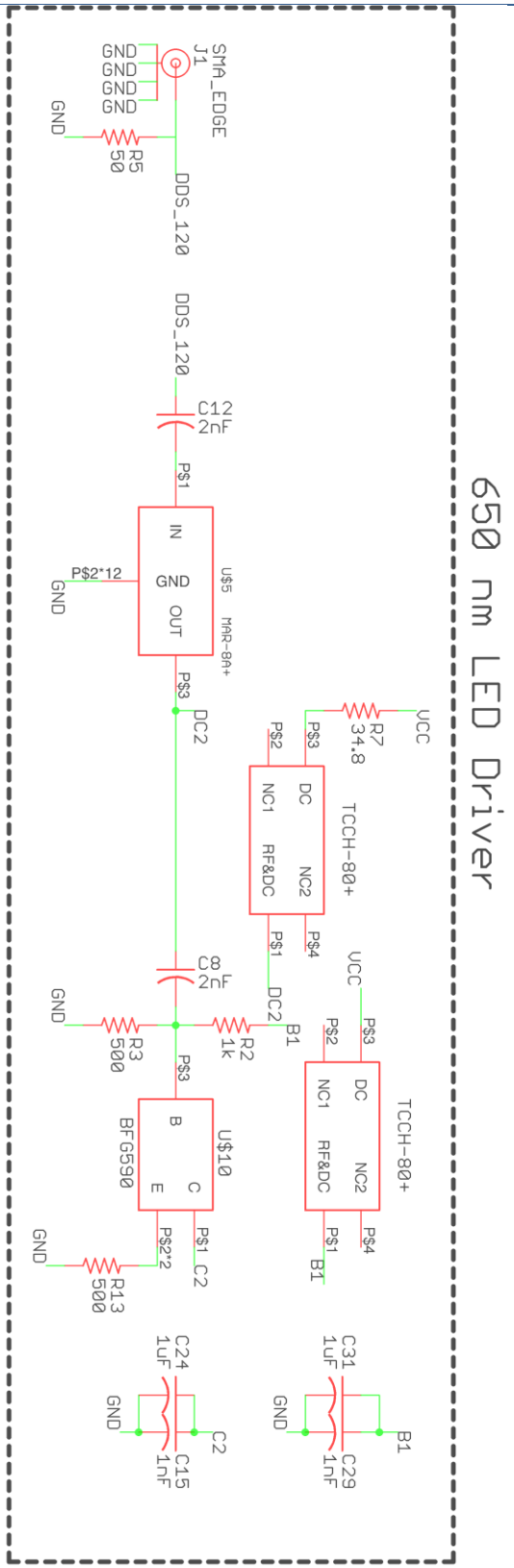

Appendix A.1.5 – BOLT-Tx Schematic (820 nm LED Driver)

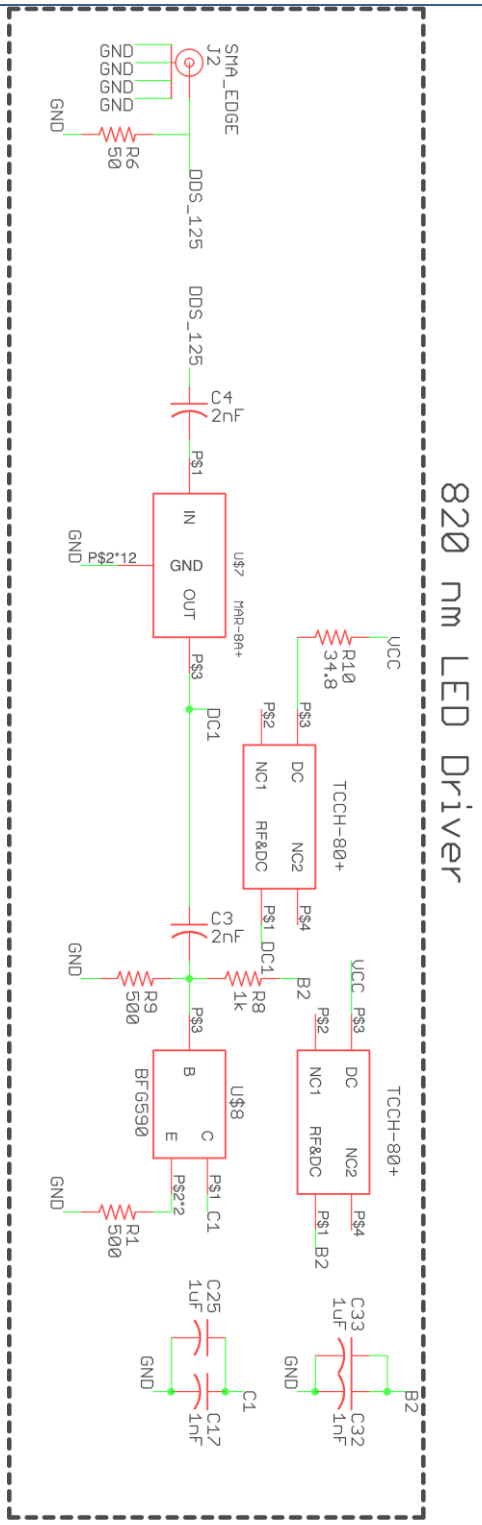

Appendix A.2.1 – BOLT-Power Schematic (Voltage Supply Inputs and Outputs)

Appendix A.2.2 – BOLT-Power Schematic (SMPS and PECL Clock Oscillator)

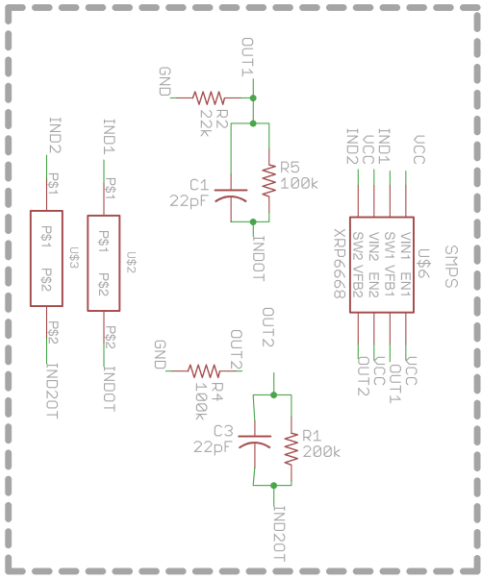

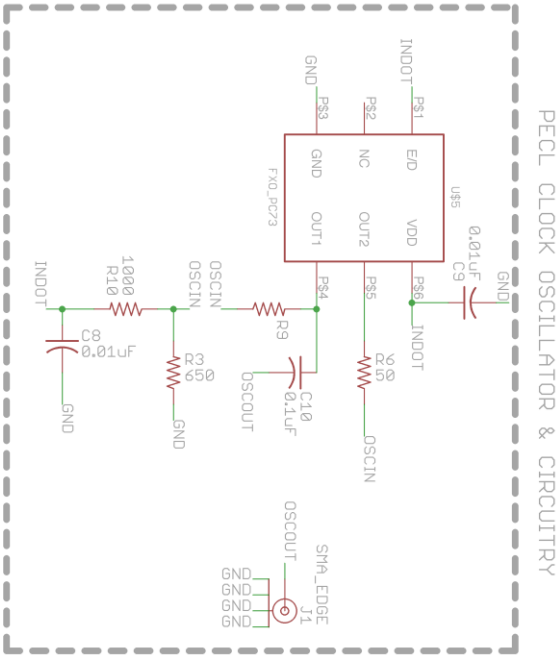

Appendix A.3.1 – BOLT-Demod Schematic (Voltage Source Inputs and Voltage References)

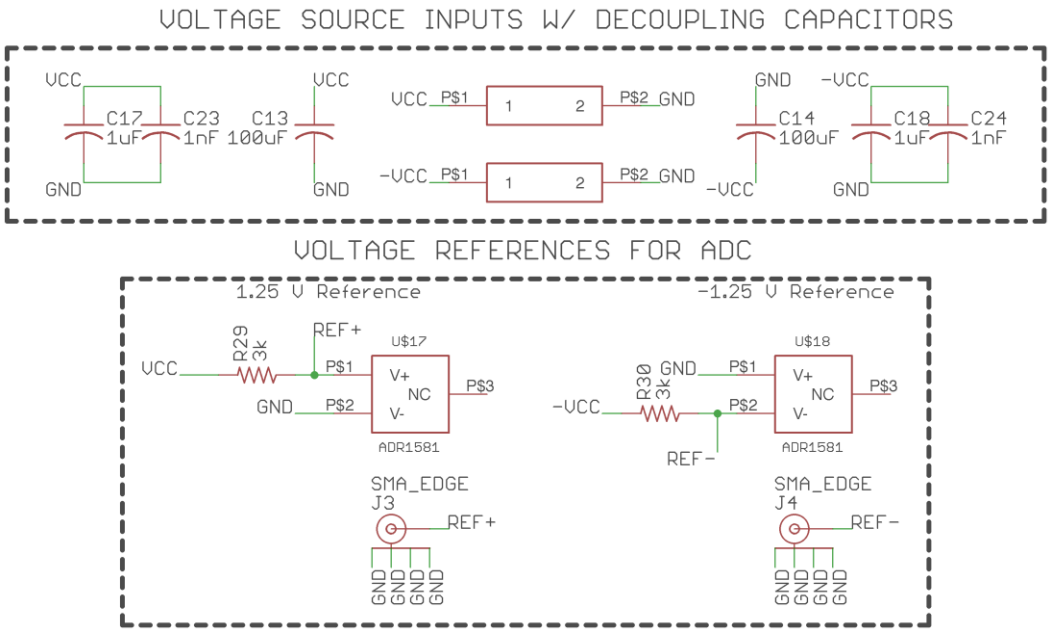

Appendix A.3.2 – BOLT-Demod Schematic (Splitters, 0-90° Hybrid and Mixers)

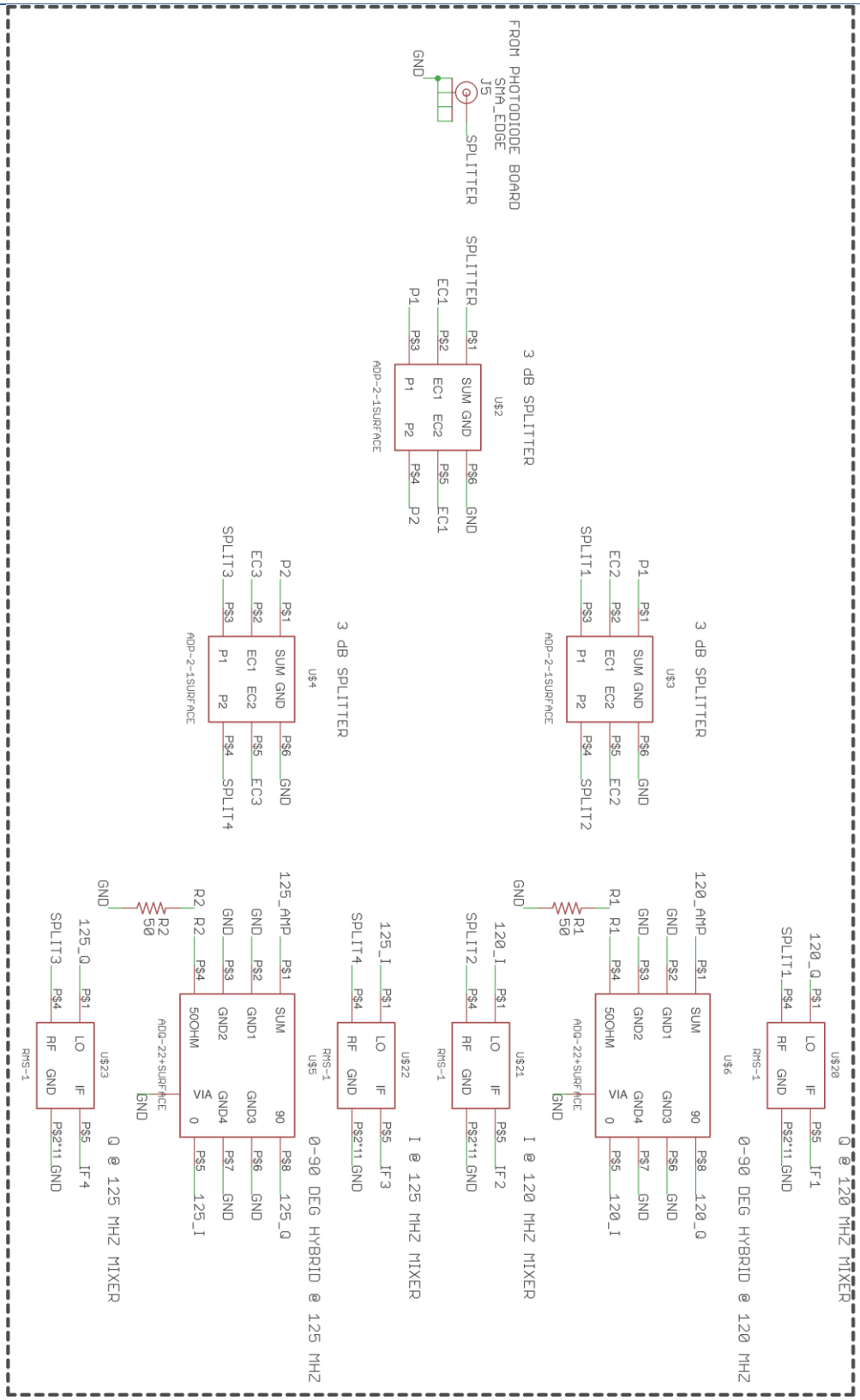

Appendix A.3.3 – BOLT-Demod Schematic (DDS Signal Amplifier with RF Choke)

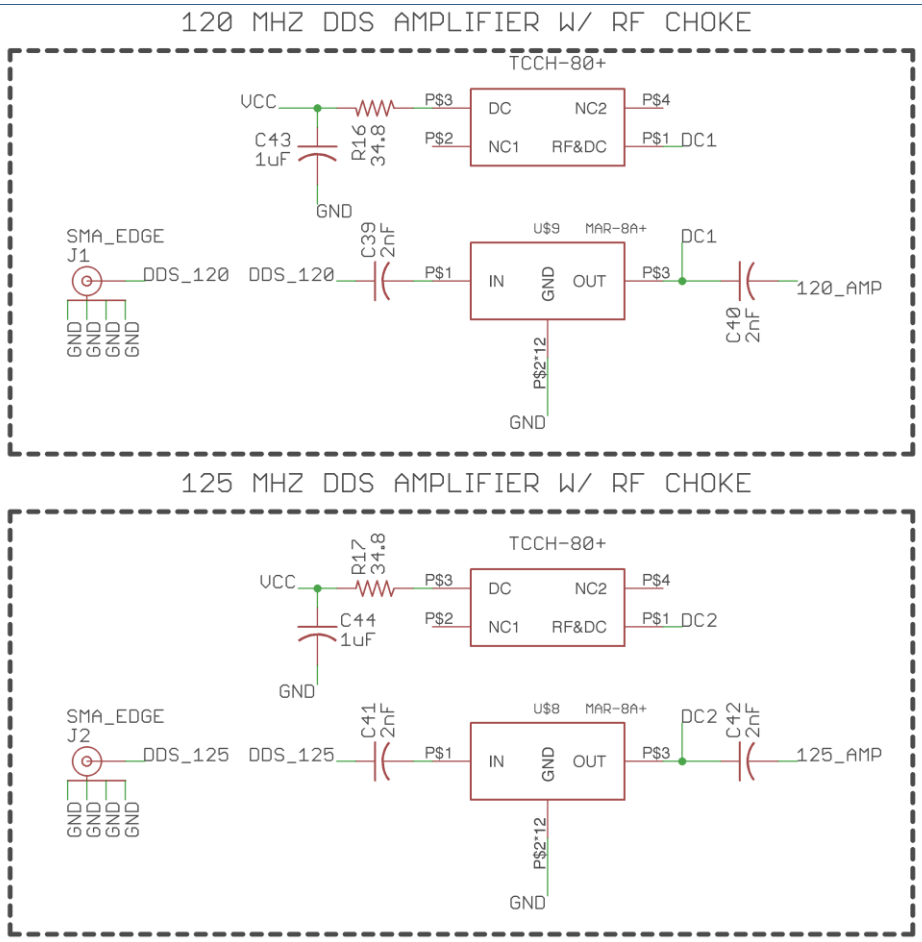

Appendix A.3.4 – BOLT-Demod Schematic (I & Q @ 120 MHz Output Channel LPF)

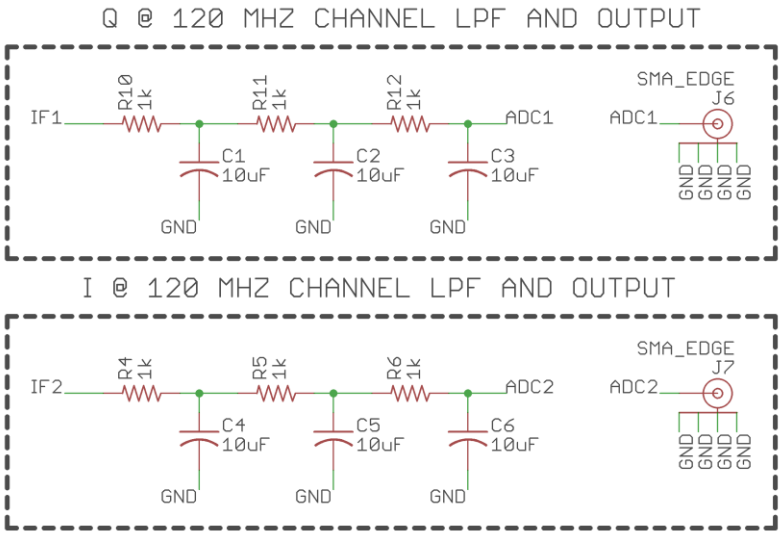

Appendix A.3.5 – BOLT-Demod Schematic (I & Q @ 125 MHz Output Channel LPF)

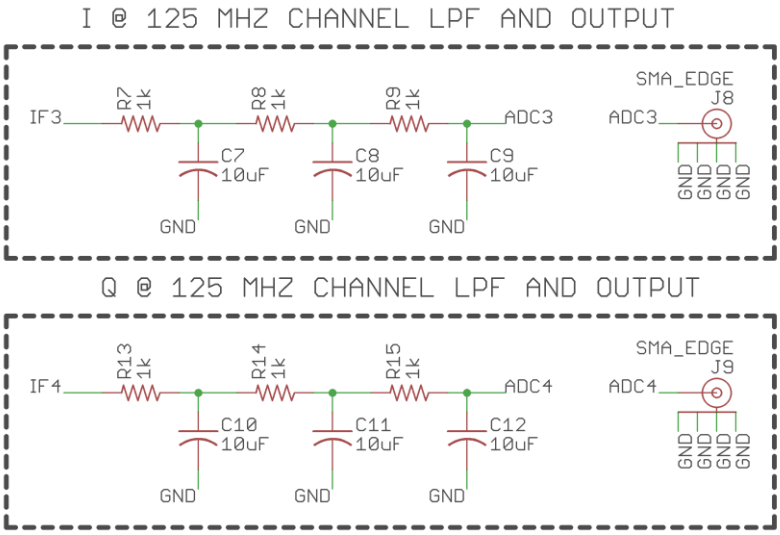

Appendix A.4.1 – BOLT-PD Schematic (Photodiode and Voltage Source Inputs)

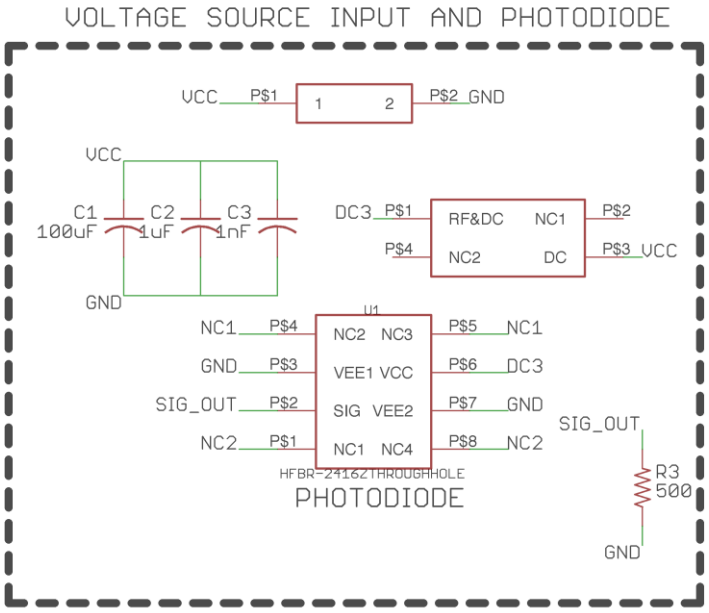

Appendix A.4.2 – BOLT-PD Schematic (Preamplifier and Band Pass Filter)

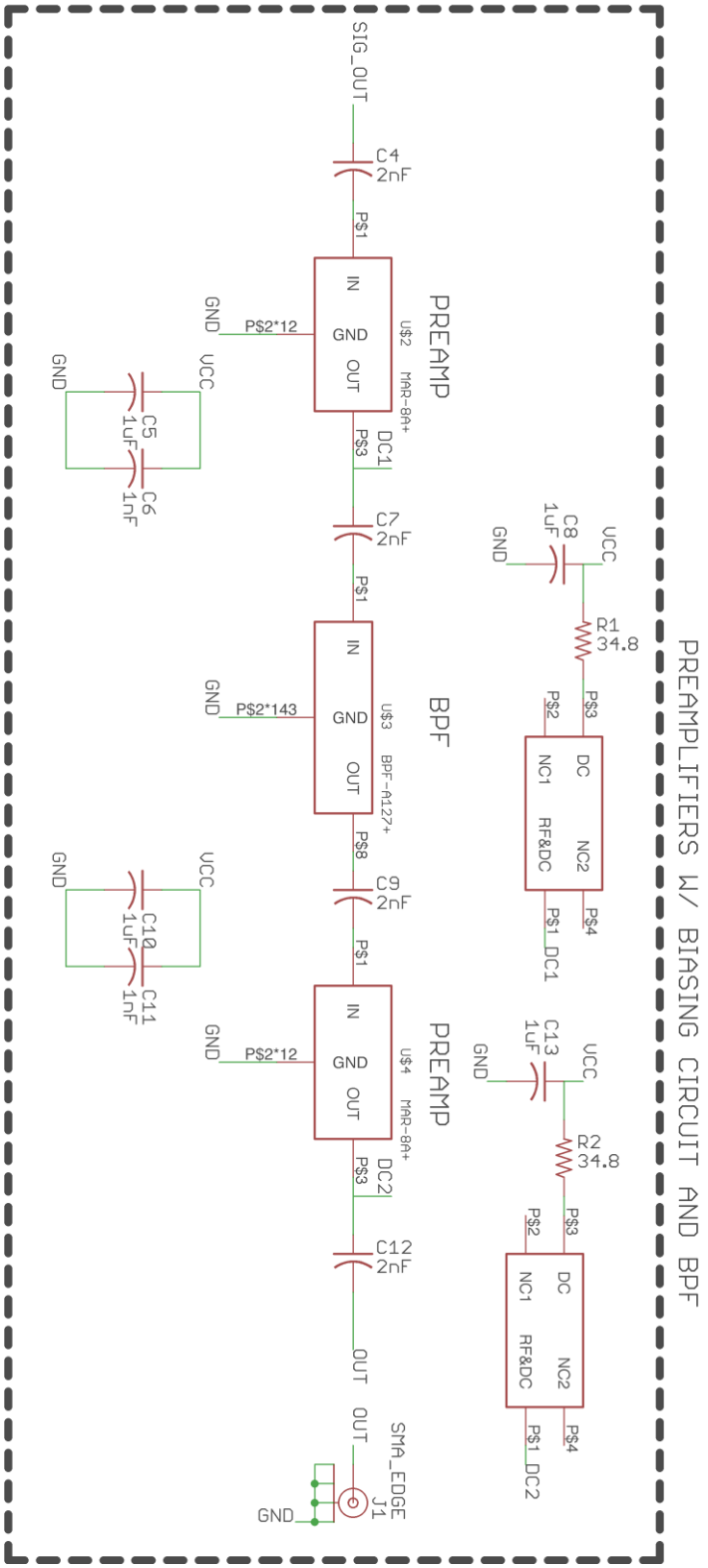

Appendix B – PCB Layouts

Appendix B.1.1 – BOLT-Tx Board Layout

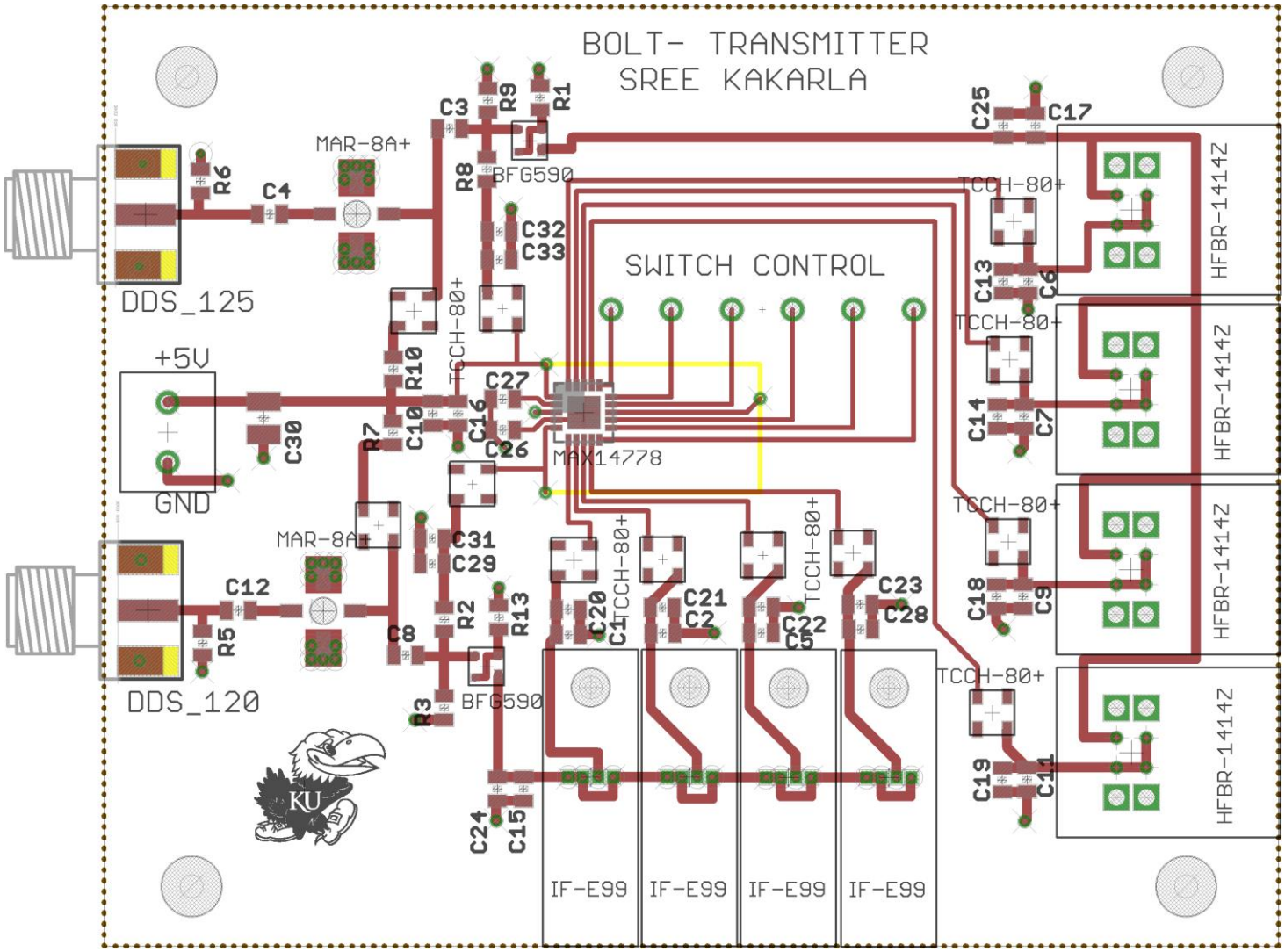

Appendix B.2.1 – BOLT-Power Board Layout

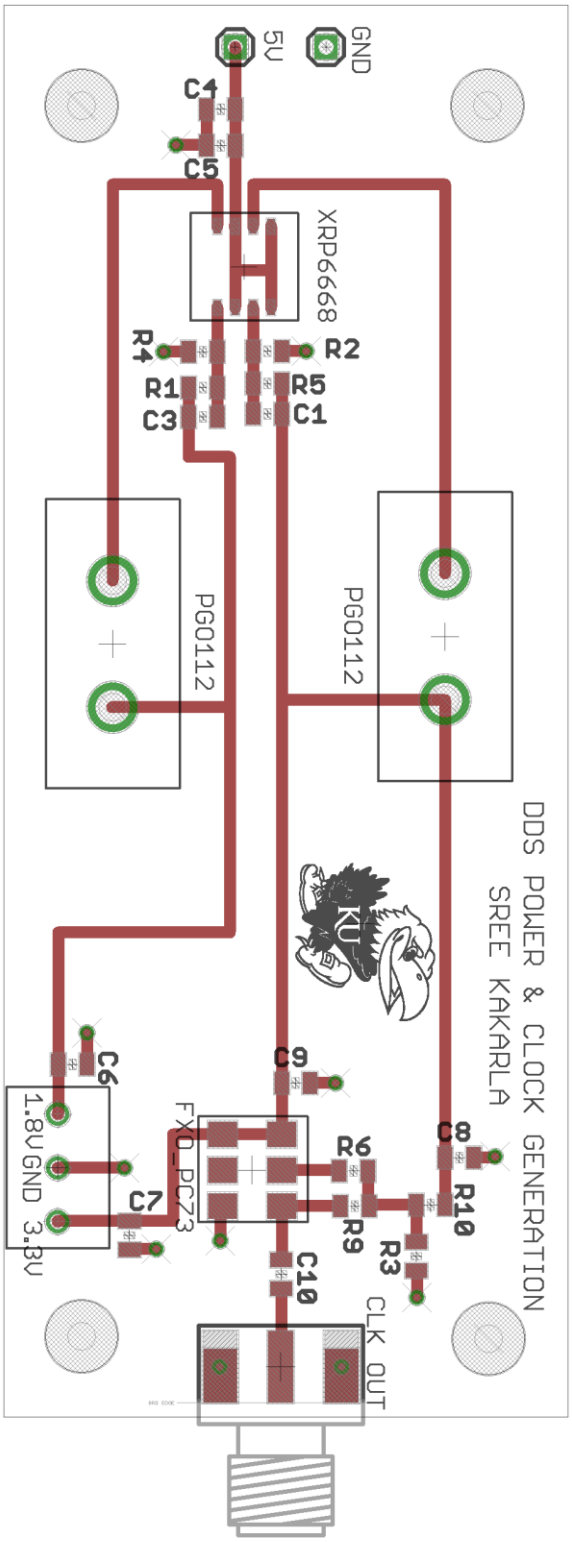

Appendix B.3.1 – BOLT-Photodiode Board Layout

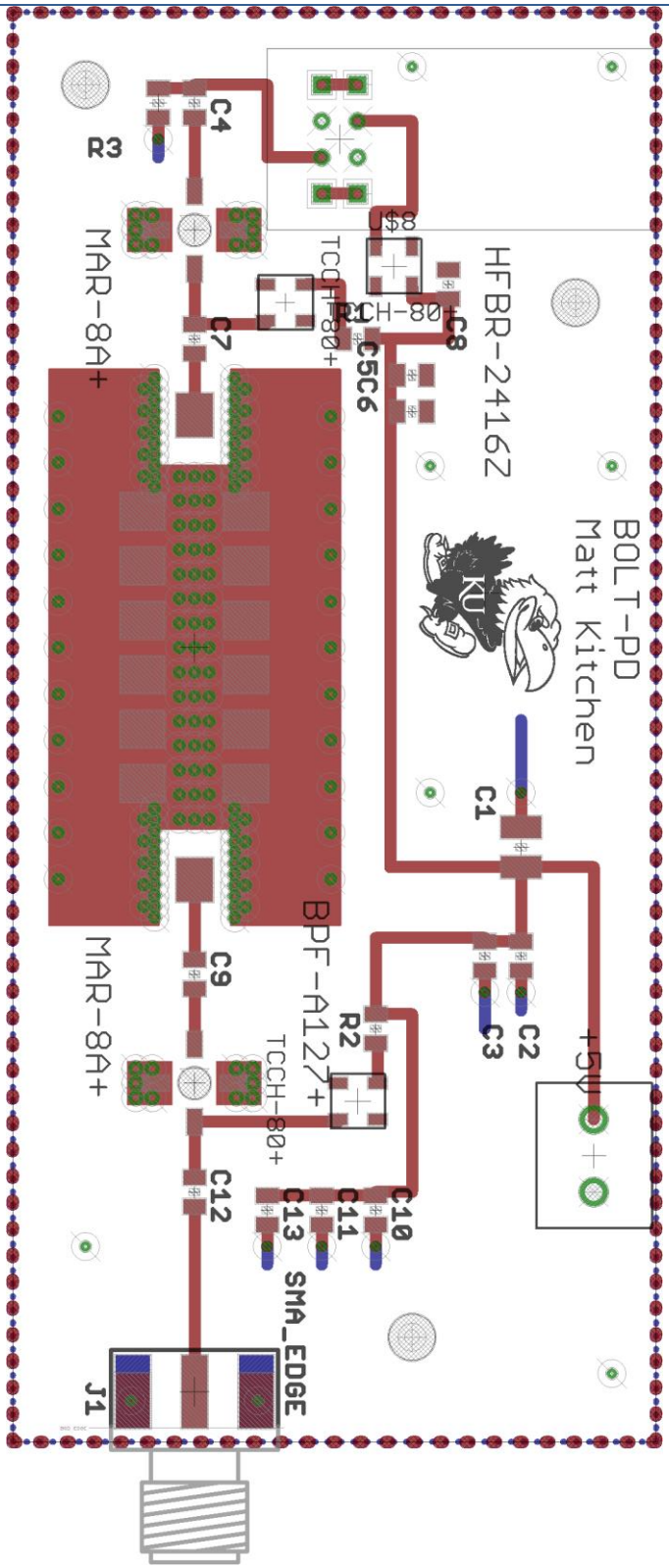

Appendix B.4.1 – BOLT-Demod Board Layout

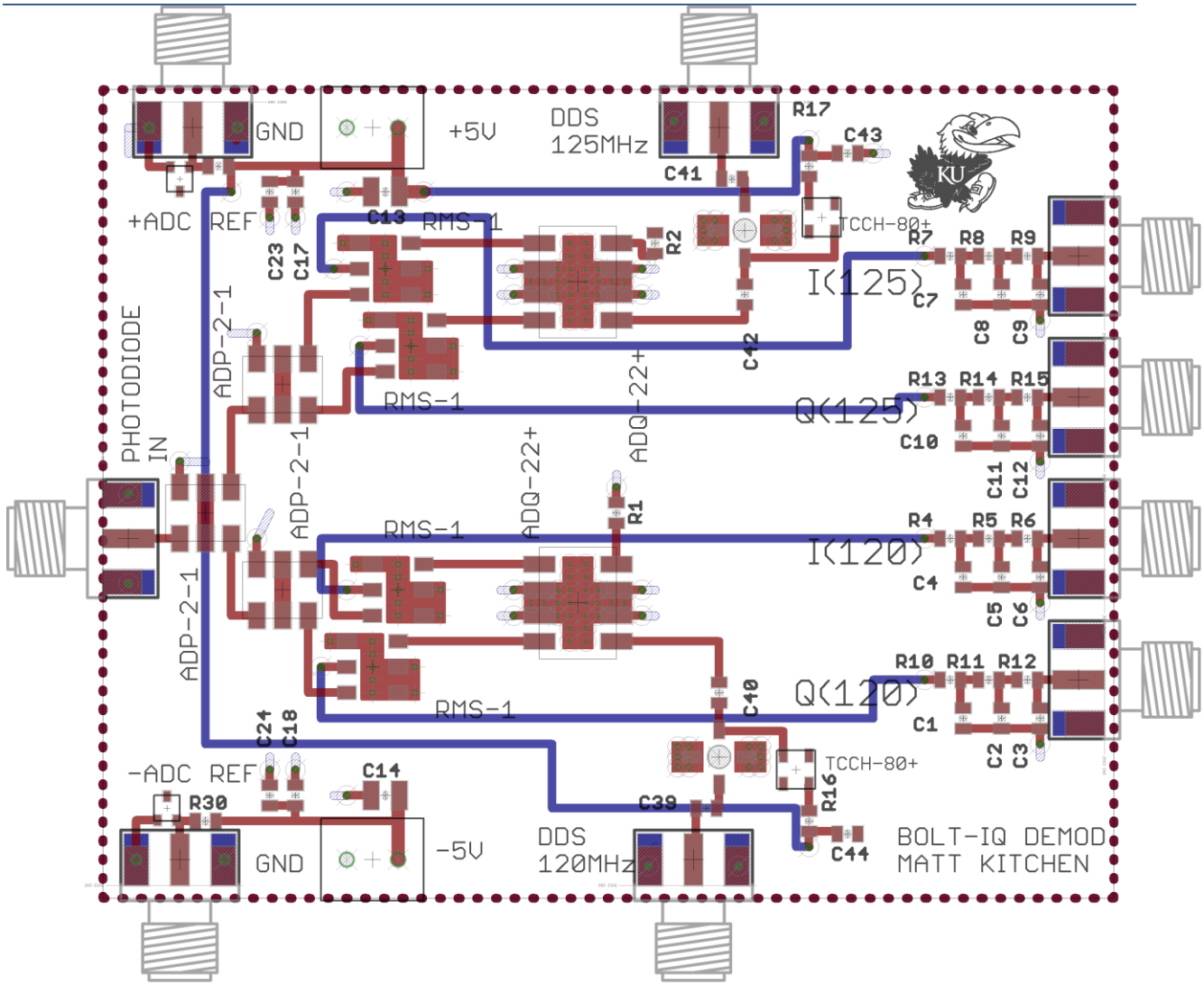

Appendix C – Component Selection Criteria and Bill of Materials

Name	Component Selected
650 nm LED	Industrial Fiber Optics Inc. P/N: IF-E99
Performance Requirements	**Selection Summary**
• Output wavelength of 650 nm • LED includes fiber optic cable connector • Capable of intensity modulation of 120 & 125 MHz	• Peak wavelength 650 nm output with a spectral bandwidth of 10 nm • Maximum optical power output of -.21 dBm • "Connector-less" style jack, allowing for quick connection or disconnection of fiber optic cable

Name	Component Selected
820 nm LED	Avago Technologies P/N: HFBR-1414Z
Performance Requirements	**Selection Summary**
• Output wavelength of 820 nm • Capable of intensity modulation of at least 120 & 125 MHz • LED includes fiber optic cable connector	• Peak wavelength 820 nm output with a spectral bandwidth of 10 nm • Maximum optical power output of -.21 dBm • Cutoff frequency of 100 MHz

Name	Component Selected
Analog Multiplexer/Switch	Maxim P/N: MAX14778
Performance Requirements	**Selection Summary**
• 2 input by 4 output switch or multiplexer • Maximum channel isolation between inputs and outputs to minimize cross-talk • Control of output channel can be selected by external source such as USB	• 4:1 multiplexer with 2 inputs (2x4:1) in a de-multiplexer configuration • -20 dB crosstalk at 100 MHz • 2 Control bits, 1 enable bit, controlled externally (outputs from an Arduino control set bits)

Name	Component Selected
Analog to Digital Converter (ADC)	Analog Devices P/N: AD7176-2 Eval. Board
Performance Requirements	**Selection Summary**
• High resolution for accurate measurement • Positive and negative voltage input • Interfaces with a PC using USB	• 24-bits of resolution • Positive and negative references can be set externally • Refer to link budget (INSERT REFERENCE FOR LINK BUDGET) for ADC sensitivity

Name	Component Selected
Bandpass Filter	Mini-Circuits P/N: BPF-A127+
Performance Requirements	**Selection Summary**
• Limit pre-amplifier bandwidth to 120 and 125 MHz as much as possible • Prevent reduction of amplifier parasitic oscillation, commonly referred to as ringing	• The bandpass filter selected has a passband frequency range of 118 to 137 MHz • Passband attenuation of ~2.75 dB • Reduces the possibility of amplifier ringing by attenuating out of band signals

Name	Component Selected
Direct Digital Synthesizer (DDS)	Analog Devices AD9959 Evaluation Board
Performance Requirements	**Selection Summary**
• Generate minimal phase-noise tones at 120 and 125 MHz • Minimal cross-talk between output channels • (4) output channels: (2) 120 MHz channels & (2) 125 MHz channels	• Versatile signal generator; capable of generating multiple waveform shapes including sine • Phase noise of • Tunable relative phase shift • Graphical User Interface

Name	Component Selected
In-Phase and Quadrature (IQ) Hybrid Splitter	Mini-Circuits ADQ-22+
Performance Requirements	**Selection Summary**
• Combiner/splitter which introduces 90° phase shift to one signal output • Insertion loss nearly 3 dB	• Phase offset of 91.27° @ 120 MHz and 91.3° @ 125 MHz • S1 loss of 3.23 & S2 loss of 3.15 @ 120 MHz

Name	Component Selected
Frequency Mixer	Mini-Circuits RMS-1+
Performance Requirements	**Selection Summary**
• Used for demodulation of AM signals at 120 & 125 MHz signals to baseband (DC) • Minimal insertion loss • Surface mount for PCB fabrication	• Conversion/Insertion Loss ~5.8 dB @ LO power of 7 dBm @ 120 & 125 MHz • LO frequency range 0 – 500 MHz and IF frequency range of 0 – 500 MHz

Name	Component Selected
Clock Oscillator (PECL)	Fox FOX-PC73
Performance Requirements	**Selection Summary**
• Clock source compatible with 50 Ohm load (DDS clock input) • Minimal jitter • 25 MHz output	• Output compatible with 50 Ohm load • ±25 ppm frequency stability • 25 MHz clock output

Name	Component Selected
Power Splitter	Mini-Circuits ADP-2-1+
Performance Requirements	**Selection Summary**
• Minimal insertion loss (over 3 dB loss from split) • Frequency range includes 120 & 125 MHz	• 3.21 dB and 3.22 dB insertion loss (.21 and .22 over 3 dB) @ 120 MHz

Name	Component Selected
RF Amplifier	Mini-Circuits MAR-8A+
Performance Requirements	**Selection Summary**
• Receiver amplifier gain of at least 30 dB • Frequency range includes 120 & 125 MHz • Surface mount • Low noise figure	• Typical gain of 31.5 dB • Frequency range DC to 1 GHz, 1 dB compression at 1 GHz • 3.1 dB noise figure @ 1 GHz

Name	Component Selected
RF Choke or Bias-T	Mini-Circuits TCCH-80+
Performance Requirements	**Selection Summary**
• Reduce RF signal couple to power supply, maximum isolation • Minimal insertion loss • Surface mount • Frequency range includes 120 & 125 MHz	• Insertion loss of .71 dB @ 100 MHz, 200 mA current • Maximum DC current of 300 mA • Recommended specifically as part of DC biasing for MAR-8A+ RF amplifier by manufacturer

Name	Component Selected
Test Sample Solution	"Phantom" (Consisting of India Ink and Water)
Performance Requirements	**Selection Summary**
• One solution with optical characteristics resembling that of oxygenated hemoglobin • Simulation of oxygenation concentration	• India ink mixed with water is commonly used as a substitute for blood in oximetry and spectrometry tests • India ink simulates variations in blood oxygenation with the water to ink mixture ratio

Name	Component Selected
BJT	NXP BFG590
Performance Requirements	**Selection Summary**
• Current amplifier used for LED signal driver • Can amplify signal frequencies of 120 and 125 MHz to current required for maximum LED intensity • Sufficient AC gain (h_{fe}) to reduce input signal power requirements	• Transition frequency of the BJT is typically 5 GHz • Maximum collector current of 200 mA • Small-signal current gain, h_{fe}, is approximately 90